5th IFQMS

The 5th International Forum
on Quantum Metrology and Sensing

PROCEEDINGS

Short Presentation Session for Young Scientists
Part 1: SE-03A

29 November, 2022
Online Conference (Zoom)

Joint Program Session with Quantum Innovation 2022

QUANTUM INNOVATION 2022

Quantum Sensing Track : Short Presentation Session for Young Scientists

SE-03A. Short Presentations Session for Young Scientists on SE-02, 04, 06, 07 Topics [5th IFQMS]

*Note: Presentation order may change within the same group.

All the times in the program are Japan Standard time (GMT+9)

Nov 29 (Tue.)	Session / Presentation	Mentor / Presenter	Affiliation	ID
13:10-14:30	**SE-03A-α1**			
	Chair	Ryota Katsumi	TUT	
	Co-chair	Naota Sekiguchi	Tokyo Tech	
	Lock-In detected ramsey magnetometry with a bulk ensemble of diamond NV centers for high-sensitivity DC-field measurement	Sena Tsuchiya	Tokyo Tech	SE-03A-α1-01
	Towards measurement of magnetic field generated by the brain of a living rat using N-V centers in diamond	Naota Sekiguchi	Tokyo Tech	SE-03A-α1-02
	Identification of current multipole sources from magnetoencephalography data	Motofumi Fushimi	UTokyo	SE-03A-α1-03
	Optimization of simultaneous measurement of magnetic field and temperature measurement by silicon vacancy quantum sensor using simultaneous resonance	Tomoaki Tanaka	QST	SE-03A-α1-04
	Spin-dependent photocarrier generation dynamics in electrically detected NV-based quantum sensor	Hiroki Morishita	Kyoto U	SE-03A-α1-05
	Towards nanoscale zero- to ultralow-field NMR	Till Lenz	JGU	SE-03A-α1-06
	Dipole-dipole interaction between NV- centers	Chikara Shinei	NIMS	SE-03A-α1-07
13:10-14:30	**SE-03A-β1**			
	Chair	Yuta Kainuma	Tokyo Tech	
	Co-chair	Naoya Morioka	Kyoto U	
	Extension of dephasing time of ensemble NV centers with a continuous-excitation protocol	Ikuya Fujisaki	Tokyo Tech	SE-03A-β1-01
	Wide temperature operation of diamond quantum sensor for electric vehicle battery monitoring	Keisuke Kubota	Tokyo Tech	SE-03A-β1-02
	A development of wearable magnetic shield for MEG	Soichiro Shido	UTokyo	SE-03A-β1-03
	Attempts to generate entanglement state between dipolar coupled NV centers created by molecular implantation	Kosuke Kimura	QST	SE-03A-β1-04
	Charge stability of shallow single NV centers in p-type diamond	Taisuke Kageura	AIST	SE-03A-β1-05
	Room-temperature electrical detection of nuclear spins in silicon carbide	Naoya Morioka	Kyoto U	SE-03A-β1-06
	(Near) zero-field cross-relaxation features for ensembles of NV centers in diamond	Omkar Dhungel	JGU	SE-03A-β1-07
13:10-14:30	**SE-03A-γ1**			
	Chair	Tomoya Sato	Tokyo Tech	
	Co-chair	Fumihiro China	NICT	
	Evaluation of a superconducting nanowire single photon detector for mid-infrared wavelengths	Satoru Mima	NICT	SE-03A-γ1-01*
	Efficient superconducting nanostrip single-photon detectors for 2 □m wavelength	Fumihiro China	NICT	SE-03A-γ1-02
	Effect of pump laser linewidth on nonlinear quantum interferometric fringes	Jasleen Kaur	Kyoto U	SE-03A-γ1-03
	Highly efficient and ultra-broadband photon pair source using chirped quasiphase matching slab waveguide matching slab waveguide	Bo Cao	Kyoto U	SE-03A-γ1-04
	Optical trapping and movement control of gold nanoparticles on an optical nanofiber	Rui Sun	Tohoku U	SE-03A-γ1-05
	Electromagnetic-field analysis of the plasmon-enhanced single photon emitters on an optical nanofiber	Yining Xuan	Tohoku U	SE-03A-γ1-06
	Ultrafast measurement of biphoton wave packets using optical Kerr gating	Takahisa Kuwana	UEC	SE-03A-γ1-07

Nov 29 (Tue.)	Session / Presentation	Mentor / Presenter	Affiliation	ID
14:50-16:10	**SE-03A-α2**			
	Chair	Naota Sekiguchi	Tokyo Tech	
	Co-chair	Ryota Katsumi	TUT	
	Growth of thick CVD diamond films containing aligned nitrogen-vacancy centers for high-sensitivity quantum sensors	Takeyuki Tsuji	Tokyo Tech	SE-03A-α2-01
	Enhancement of fluorescence collection efficiency using angle-shaped diamonds for compact magnetic sensor	Yuta Shigenobu	Tokyo Tech	SE-03A-α2-02
	Transfer-printing-based integration of SiN grating structure on diamond toward highly sensitive quantum sensor	Ryota Katsumi	TUT	SE-03A-α2-03
	NVC-SPM system to inspect electric devices	Teruo Kohashi	Hitachi	SE-03A-α2-04*
	Enhancing sensitivity with entanglement in coupled nitrogen vacancy centres	Ernst David Herbschleb	Kyoto U	SE-03A-α2-05
	Frequency-bin generation of entangled photons via quantum optical synthesis	Takeru Naito	UEC	SE-03A-α2-06
	Development of highly sensitive gravimeter based on atom interferometry using hybrid system for field applications	Takeshi Hojo	UEC	SE-03A-α2-07
14:50-16:10	**SE-03A-β2**			
	Chair	Naoya Morioka	Kyoto U	
	Co-chair	Yuta Kainuma	Tokyo Tech	
	Implementation of double quantum magnetometry to continuously excited ramsey method	Yuta Araki	Tokyo Tech	SE-03A-β2-01
	Development of highly sensitive compact quantum sensor with NV center in 12C-enriched CVD diamond for bio-medical and industrial application	Yuta Kainuma	Tokyo Tech	SE-03A-β2-02
	Development of a nonmagnetic helical sensor drive multipoint measuring mechanism for magnetocardiography in animals	Wenyu Shang	UTokyo	SE-03A-β2-03
	Ensemble NV- center in diamond for quantum sensing created by high fluence electron beam irradiation	Shuya Ishii	QST	SE-03A-β2-04
	Synthesis of n-type diamond using tert-butyl phosphine for high sensitivity of the NV sensor	Riku Kawase	Kyoto U	SE-03A-β2-05
	Decoherence phenomena in nitrogen-vacancy diamond	Aulden Jones	Georgia Tech	SE-03A-β2-06
14:50-16:10	**SE-03A-γ2**			
	Chair	Fumihiro China	NICT	
	Co-chair	Tomoya Sato	Tokyo Tech	
	Improvement in the long-term stability of the interferometer gyroscope using slow and continuous atomic beams	Naoki Nishimura	Tokyo Tech	SE-03A-γ2-01
	Bragg interferometer using slow and continuous atomic beam with sub-recoil transverse momentum width	Tomoya Sato	Tokyo Tech	SE-03A-γ2-02*
	Development of a cryogenic suspension system for TOrsion-Bar Antennae (TOBA)	Ching Pin Ooi	UTokyo	SE-03A-γ2-03
	Torsion-bar antenna for early earthquake alert	Yuka Oshima	UTokyo	SE-03A-γ2-04
	Optimized Design of Quasi-phase-matched crystal for Spectrally-Pure-State Generation at MIR Wavelengths Using Metaheuristic Algorithm	Wu-Hao Cai	Tohoku U	SE-03A-γ2-05
	Experimental generalized measurement of qubits using a quantum computer	Tingrui Dong	Tohoku U	SE-03A-γ2-06

Note: This program was created for fostering young scientists. Presentations with asterisks (*) are excluded from awarding.

Lock-In Detected Ramsey Magnetometry with a Bulk Ensemble of Diamond NV Centers for High-Sensitivity DC-Field Measurement

Sena Tsuchiya[1], Daisuke Nishitani[1], Yusei Aoki[1], Takeharu Sekiguchi[1], Takayuki Shibata[2], Takayuki Iwasaki[1], and Mutsuko Hatano[1,3]

[1]*Department of Electrical and Electronics Engineering, School of Engineering, Tokyo Institute of Technology*

[2]*DENSO CORPORATION*

[3]*National Institutes for Quantum Science and Technology*

tsuchiya.s.ag@m.titech.ac.jp

Introduction

Nitrogen-vacancy (NV) centers in diamond have attracted much attention as high sensitivity quantum magnetic sensors that can be operated at room temperature. Our group has demonstrated magnetocardiography of living rats by combining continuous-wave optically detected magnetic resonance (CW-ODMR) with lock-in (LI) detection[1]. However, further improvement of DC-field sensitivity is necessary to detect magnetoencephalography signals. Double-quantum (DQ) Ramsey magnetometry[2] based on pulsed ODMR scheme is expected to achieve much higher sensitivity by improving both spin dephasing time T_2^* and contrast[2]. Combination with LI detection of fluorescence intensity should reduce noise, remove signal offset, and allow real-time measurement. In this study, we implemented LI detection under pulsed optical excitation and detection with DQ Ramsey sequences to demonstrate the sensitivity improvement.

Methods

The diamond sample used was grown by HPHT with ^{12}C-enriched source in NIMS, and the NV centers were created by electron beam irradiation (1×10^{17} cm^{-2}) and annealing in QST. The concentrations of NV and P1 (substitutional nitrogen) centers were 0.05 ppm and 1.1 ppm. Fig. 1(a) shows our experimental setup. Pulsed optical excitation at 532 nm and the DQ-4-Ramsey sequence[2] with resonant dual-frequency microwave (MW) were applied to a bulk ensemble of NV centers in diamond. The illumination volume was roughly ($60\times160\times470$) μm^3. The fluorescence signal modulated by the DQ-4-Ramsey sequence was detected and demodulated by a LI amplifier. The MW pulse width (0.22 μs) for this sequence was calibrated from the DQ-Rabi oscillation measurements.

Results and discussion

Fig. 1(b) shows the LI detected DQ-4-Ramsey fringes with microwave frequencies tuned to the central resonance of the ^{14}N hyperfine triplet. The inset FFT spectrum shows clearly this triplet structure with the splitting doubled by the DQ sequence. Fig. 1(c) shows MW frequency dependence of the Ramsey signal at a fixed free-precession time τ using the SQ(single quantum)-2-Ramsey[2] and DQ-4-Ramsey sequences. The DQ-4-Ramsey signal exhibits a 15% steeper slope than the SQ-2-Ramsey signal. The magnetic field sensitivity can be estimated from repeated measurements of the Ramsey signal with a fixed $\Delta\nu$ at the steepest slope. We will discuss the sensitivity improvement factors such as lock-in detection for enhancing signal-to-noise ratio and DQ-4-Ramsey sequence for the Ramsey slope improvement.

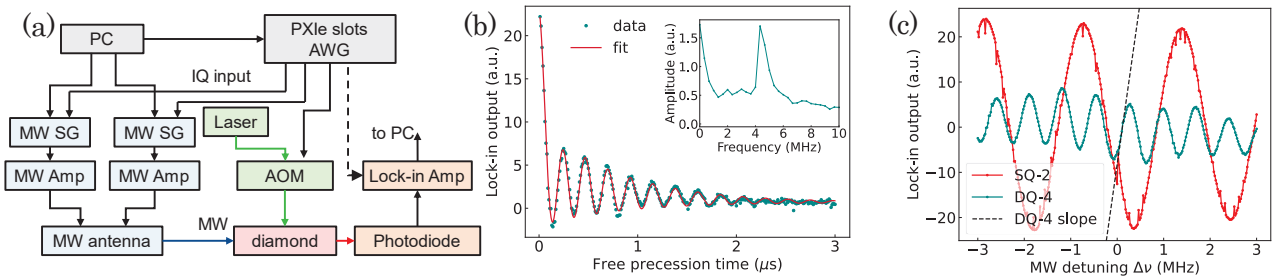

FIG. 1. (a) Experimental set up for LI detected Ramsey measurements. (b) DQ-4-Ramsey signal by LI detection at frequency detuning of $\Delta\nu = 0.0$ MHz, in the time domain and frequency domain (inset). (c) Detuning sweep of the LI detected DQ-4-Ramsey ($\tau = 0.46$ μs) and SQ-2-Ramsey ($\tau = 0.40$ μs). The dashed line represents the steepest slope of the DQ-4-Ramsey signal.

Acknowledgement

This work was supported by MEXT Q-LEAP Grant Number JPMXS0118067395. We thank Dr. M. Miyakawa, Dr. T. Taniguchi (NIMS), Dr. S. Ishii, S. Saiki, and S. Onoda (QST) for providing the diamond sample.

Reference

[1]K. Arai et al., Commun. Phys. **5**. 200 (2022). [2]C. A. Hart et al., Phys. Rev. Appl. **15**, 044020 (2021).

Towards measurement of magnetic field generated by the brain of a living rat using *N*-V centers in diamond

Naota Sekiguchi[1], Motofumi Fushimi[2], Ken-ichi Kajiyama[1], Ryoma Matsuki[1], Takayuki Iwasaki[1], Masaki Sekino[2], and Mutsuko Hatano[1]

[1]*Department of Electrical and Electronics Engineering, Tokyo Institute of Technology, Tokyo 152-8552, Japan*
[2]*Department of Bioengineering, University of Tokyo, Tokyo 113-8656, Japan*
Sekiguchi.n.ac@m.titech.ac.jp

Measurement of a biomagnetic field is of great importance to understand neuron activities in a living body. Ultrasensitive magnetometers such as superconducting quantum interference device sensors and optically-pumped atomic magnetometers have successfully measured a magnetic field generated by an internal organ including brain and been applied to clinical diagnosis. While these conventional magnetometers exhibit extreme field sensitivity of the order of $\mathrm{fT}/\sqrt{\mathrm{Hz}}$, spatial resolution is limited to centimeters due to intrinsic structures of those sensor heads. Recently, diamond quantum sensor based on negatively charged nitrogen-vacancy (*N*–V) centers has attracted much attentions because of its high spatial resolution. Good field sensitivity of $15\ \mathrm{pT}/\sqrt{\mathrm{Hz}}$ at low frequency has been demonstrated using an ensemble of *N*–V centers [1], and *N*–V center based magnetocardiography of a living rat [2] with millimeter-scale resolution has been reported. Magnetoencephalography (MEG) using *N*–V centers, however, has not been realized and requires a field sensitivity on the order of $\mathrm{pT}/\sqrt{\mathrm{Hz}}$. We develop a sensitive diamond magnetometer based on a *N*–V center ensemble for MEG of a living rat.

Figure 1 shows our experimental setup. A rat was anesthetized and laid on a warm bed. Electrocardiogram of the rat was monitored using electrodes sticked into limbs. We stimulated the somatosensory of the rat by applying current pulses with 300-μs width and repetition frequency of about 4 Hz via another electrode sticked into a hind limb. This stimulation is supposed to generate a somatosensory evoked field (SEF) from the brain of the rat, which can be detected with a quantum diamond sensor above the rat head. The single-crystalline diamond was synthesized by a temperature-gradient method under high-pressure and high-temperature. *N*–V centers were produced by electron beam irradiation followed by high-temperature annealing in vacuum. We used an optically-detected magnetic resonance signal of *N*–V center ensemble that oriented along the *z* axis. A linearly polarized laser light of 532 nm illuminated the diamond. A small portion of the laser beam was picked up to compensate the intensity fluctuation. Fluorescence from the diamond was collected by a lens and detected by a photodiode. A bias magnetic field of about 1 mT generated by a ring permanent magnet was applied to the diamond along the *z* axis to sufficiently split the $|\pm 1\rangle$ ground states. The magnetic resonance between $|0\rangle \leftrightarrow |\pm 1\rangle$ was induced by a frequency modulated microwave (MW) field: sidebands resonant to the hyperfine states were generated by mixing an RF with the MW; the career frequency of MW was modulated at around 10 kHz to adopt a lock-in technique. The acquired signal was accumulated in accordance with the stimulation pulses. We will discuss the present situation including the noise floor and detectable field in the short presentation.

This work was supported by MEXT Q-LEAP Grant Number JPMXS0118067395.

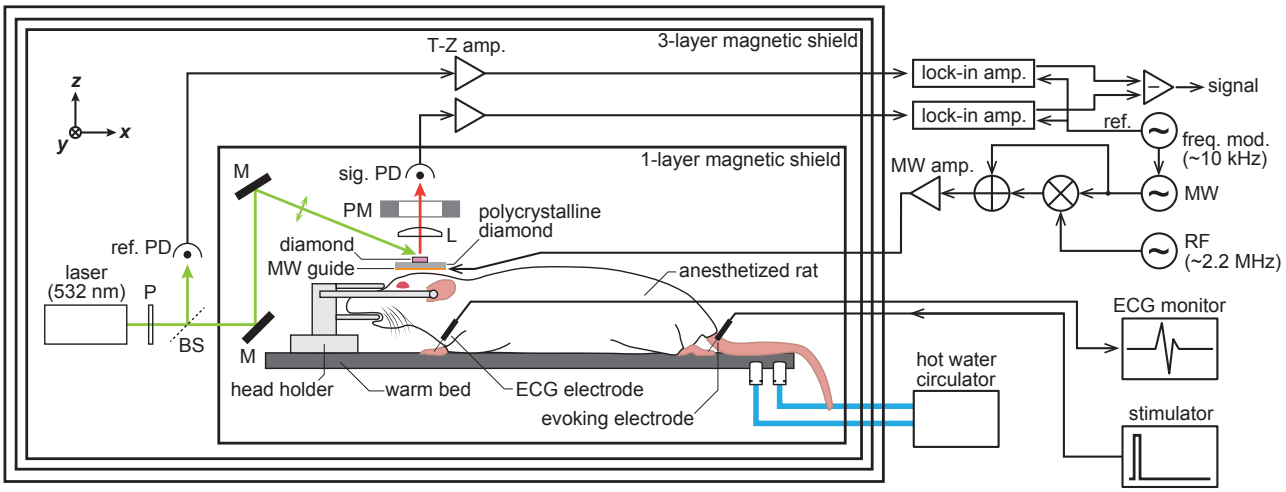

FIG 1. Experimental setup. P: polarizer; BS: beam splitter; PD: photodiode; M: mirror; L: lens; PM: permanent magnet; T-Z amp.: transimpedance amplifier.

[1] J. F. Barry *et al*., Proc. Natl. Acad. Sci. **113**, 14133 (2016).

[2] K. Arai *et al*., Commun. Phys. **5**, 200 (2022).

Identification of current multipole sources from magnetoencephalography data

Motofumi Fushimi[1], Mutsuko Hatano[2], Takaaki Nara[3], and Masaki Sekino[1]
[1]*Department of Bioengineering, Graduate School of Engineering, The University of Tokyo*
[2]*Department of Electrical and Electronics Engineering, School of Engineering, Tokyo Institute of Technology*
[3]*Department of Information Physics and Computing, Graduate School of Information Science and Technology, The University of Tokyo*
motofumi-fushimi@g.ecc.u-tokyo.ac.jp

Introduction

In magnetoencephalography (MEG) source identification, current sources are typically modeled as equivalent current dipoles (ECDs). However, actual neural sources have non-negligible spatial pattern, which can be accounted for using equivalent current multipoles (ECMs). We extend the previously proposed algebraic method for the multipole source identification in the two-dimensional (2D) case [1] to the three-dimensional (3D) case to enhance applicability of the framework to the realistic MEG problem. This can also be seen as an extension of the 3D dipole and dipole-quadrupole identification method [2] to general-order multipoles.

Methods

By adopting the concentric sphere head model, the radial component of the magnetic field is represented by the current source according to the Biot-Savart law as shown in Fig. 1. The multipole expansion of the equation relates the unknown multipole source parameters (location and moment) to the MEG data [3]. We derived an algebraic equation for multipole parameters, the detail of which will be shown in the presentation. We validated the proposed method by numerical simulations with two distinct current quadrupoles and octupoles.

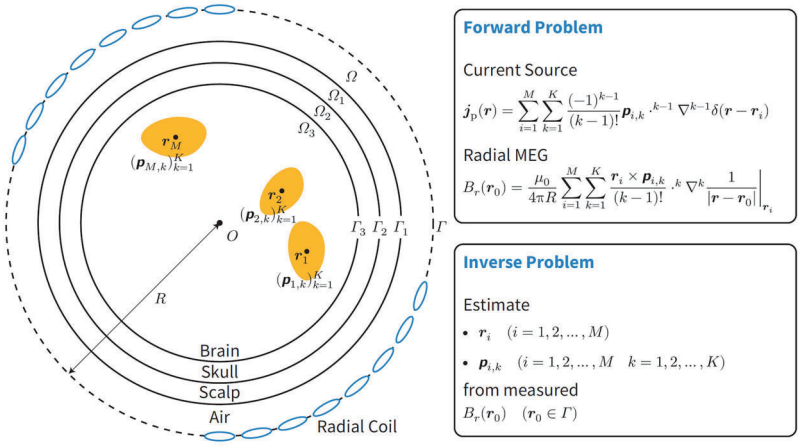

FIG. 1. Problem formulation of the MEG current source identification in the present study.

Results and Discussion

The proposed method could stably estimate both the two quadrupoles and octupoles, which has not been achieved in previous methods, validating the efficacy of the method. In contrast, the results of the ECD model had huge errors because the ECD model erroneously tries to explain MEG data resulting from multipoles by dipoles. The resulting figures will also be presented in the conference.

Acknowledgements

This work was supported by MEXT Q-LEAP Grant Number JPMXS0118067395.

Reference

[1]T. Nara *et al.*, *Phys. Med. Biol.*, 52(13), 3859-3879 (2007).
[2]T. Nara *et al.*, *Math. Probl. Eng.*, 2013, 413980 (2014).
[3]G. Nolte *et al.*, *Biophys. J.*, 73(3), 1253-1262 (1997).

Optimization of simultaneous measurement of magnetic field and temperature measurement by silicon vacancy quantum sensor using simultaneous resonance

Tomoaki Tanaka[1], Yuichi Yamazaki[1], Kazutoshi Kojima[2], and Takeshi Ohshima[1]
[1]*National Institutes for Quantum Science and Technology*
[2]*National Institute of Advanced Industrial Science and Technology*
tanaka.tomoaki@qst.go.jp

Background and Purpose

Silicon vacancies (V_{Si}) in silicon carbide (SiC) have attracted great attention because we can measure magnetic field and temperature in some devices by fabricating V_{Si} in the devices[1,2]. Simultaneous measurement of magnetic field and temperature using SiC-V_{Si} quantum sensor requires simultaneous Optically Detected Magnetic Resonance (ODMR) measurement of the ground and excited states. However, the ODMR contrast (= sensitivity) of the excited state is about one order of magnitude smaller than that of the ground state. So, the temperature measurement is time-consuming. To solve this problem, we have proposed and demonstrated a new temperature measurement method, Simultaneous Resonance (SR) ODMR, which based on the modulation of the ODMR contrast of the ground state by simultaneous resonance of the ground and excited states[3]. This method converts part of the contrast of the ground state into that of the excited state. It is necessary to optimize the RF power ratio which is related to the contrast ratio between the ground and excited states to minimize the measurement time in magnetic field and temperature (SR) simultaneous measurement. Therefore, the purpose of our study is to optimize the power ratio of the RF using the simultaneous measurement by SR ODMR.

Methods and Results

V_{Si} dots were fabricated on p-type 4H-SiC epitaxial thin film (5.6 μm) using a particle beam writing (ion species: He, energy: 0.5 MeV, irradiation dose: 3×10^5 /dots). The size and depth of the dots are 5×5 μm^2 and ~1 μm, respectively. Three signal generators were used for the measurements, one fixed at the resonance frequency of the ground state (70 MHz) for SR, and the others swept near those of the ground and excited states (20-170, 300-600 MHz) for the ground state and SR ODMR measurements, respectively.

Figure 1 shows the spectra of ground and SR excited states by ODMR simultaneous measurements. Signal intensities indicated by red and blue arrows are observed. The former is a resonance of the ground state, and the latter is that of the excited states. We can find that another dip indicated by green arrow around 500 MHz exists. The sweep condition indicates that this frequency corresponds to 70 MHz of the ground state measurement. This suggests that the resonance of the ground state occurs in both the ground state and SR ODMR measurements. As a result of their competition, the dip appears at around the 500 MHz on the SR ODMR side. We measured the changing of ODMR contrast of the ground and excited states when we change the RF power of signal generators. The signal intensity was almost the same at the RF power ratio of 1:9 for SR and ground state ODMR. At this condition, the contrast of SR is more than four times that of traditional excited state measurement. This suggests that we achieved faster measurement than conventional simultaneous ground and excited states measurement.

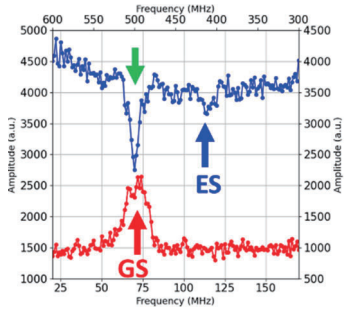

FIG. 1. Simultaneous ODMR measurement of ground and SR excited states (GS and ES) spectra.

Acknowledgement

This work was supported by MEXT Q-LEAP Grant Number JPMXS118067395, ATLA Grant number JPJ004596, and KAKENHI Grant Number 20H00355, 21H04553.

Reference

[1]M. Niethammer *et al.*, Phys. Rev. Appl. **6**, 034001 (2016).
[2]T. M. Hoang *et al.*, Appl. Phys. Lett. 118, 044001 (2021).
[3]Y. Yamazaki *et al.*, The 69th JSAP Spring Meeting, 25a-E301 (2022).

Spin-Dependent Photocarrier Generation Dynamics in Electrically Detected NV-Based Quantum Sensor

Hiroki Morishita,[1,2] Naoya Morioka,[1,2] Tetsuri Nishikawa,[1,3] Hajime Yao,[1,3]
Shinobu Onoda,[4] Hiroshi Abe,[4] Takeshi Ohshima,[4] and Norikazu Mizuochi[1,2]
[1] *Institute for Chemical Research, Kyoto University, Gokasho, Uji, Kyoto 611-0011, Japan.*
[2] *Center for Spintronics Research Network, Institute for Chemical Research, Kyoto University, Gokasho, Uji, Kyoto 611-0011, Japan.*
[3] *Department of Molecular Engineering, Graduate School of Engineering, Kyoto University, Nishikyo-Ku, Kyoto, Kyoto, 615-8510, Japan.*
[4] *National Institutes for Quantum Science and Technology, Takasaki, Gunma, 370-1292, Japan.*
h-mori@scl.kyoto-u.ac.jp

A nitrogen-vacancy (NV) center in diamond is a promising candidate for room-temperature quantum sensors thanks to its long electron spin coherence in ambient conditions [1]. In previous demonstrations, the NV electron spin was detected optically, but another method called photoelectrically detected magnetic resonance (PDMR) is attracting attention. The PDMR technique can read out NV electron spin [2-6] and coupled nuclear spins [7,8]. The electrical detection technique is advantageous for developing and integrating quantum sensors and other quantum devices [7]. However, the mechanism for the electrical detection of NV spins is not fully understood. In this study, we perform the pulsed PDMR measurements using the ensemble of NV centers (concentration of ~ 1.4 $\times 10^{17}$ cm^{-3}) created by 2 MeV electron irradiation with a fluence of 1×10^{17} cm^{-2} at 745 °C, followed by annealing at 1000 °C for 1 h in an argon atmosphere. We observe positive contrast in PDMR (Fig. 1(a)) even though a negative PDMR contrast is usually observed. To discuss the sign of the PDMR contrast, we numerically analyze the dynamics of photocarrier generation by NV centers using a seven-level rate model. We found that the sign of the PDMR contrast depends on the difference in the photocurrent generated from the excited states and the metastable state of NV centers.

Furthermore, we demonstrate AC magnetic field sensing using spin coherence with the PDMR technique. AC magnetic field measurement with the PDMR technique is still challenging because the noise from a fluctuating magnetic environment is greater than the measured signal. Using a phase-cycling-based noise-canceling technique to suppress the noise, we demonstrate AC magnetic field sensing with the PDMR technique (Fig. 1(b)). We observe electrically detected AC magnetic field sensing with a sensitivity of ~29 nT/$\sqrt{\text{Hz}}$. In this talk, we will discuss the mechanism of the NV center's electrical detection and the sensitivity of the electrically detected AC magnetic field sensing.

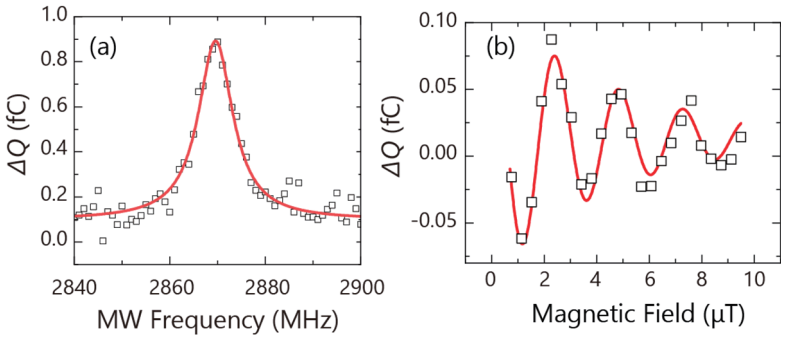

FIG.1 (a) Pulsed PDMR spectrum. (b) AC magnetic field sensing with the PDMR technique

Acknowledgments

We thank T. Ono, T. Moriyama, and Y. Shiota for their technical help. This work was supported by MEXT Q-LEAP (No. JPMXS0118067395), KAKENHI (No. 19H02546), and Kyoto University Nano Hub.

Reference

[1] E. D. Herbschleb et al., *Nat. Commun.* 10, 3766 (2019). [2] E. Bourgeois et al., *Nat. Commun.* 6, 8577 (2015).
[3] F. M. Hrubesch et al., *Phys. Rev. Lett.* 118, 037601 (2017). [4] M. Gulka et al., *Phys. Rev. Applied* 7, 044032 (2017)
[5] P. Siyushev et al. *Science* 363, 728 (2019). [6] T. Murooka et al., *App. Phys. Lett.* 118, 253502 (2021).
[7] H. Morishita et al., *Sci. Rep.* 10, 792 (2020). [8] M. Gulka et al., *Nat. Commun*, 12, 4421 (2021).

Towards nanoscale zero- to ultralow-field NMR

Till Lenz[1,2*], Omkar Dhungel[1,2], Arne Wickenbrock[1,2], Lykourgos Bougas[1], John W. Blanchard[2,3], Gopalakrishnan Balasubramanian[4], Anjusha Vijayakumar Sreeja[5], Fedor Jelezko[5], and Dmitry Budker[1,2,6]

[1]*Johannes Gutenberg-Universität Mainz, 55128 Mainz, Germany*
[2]*Helmholtz Institut Mainz, 55099 Mainz, Germany*
[3]*Quantum Technology Center, University of Maryland, College Park, Maryland 20742, USA*
[4]*Helmholtz-Zentrum Dresden-Rossendorf (HZDR), Bautzner Landstr. 400, 01328 Dresden*
[5]*Institute for Quantum Optics, Ulm University, Albert-Einstein-Allee 11,89081 Ulm, Germany*
[6]*Department of Physics, University of California, Berkeley, California 94720-7300, USA*
**tilllenz@uni-mainz.de, presenter*

Abstract: Nuclear magnetic resonance (NMR) is a widely used tool in chemical analysis as well medical diagnostics. While medical diagnostics is the most prominent branch of the NMR subfield magnetic resonance imaging (MRI), chemical analysis is usually performed without imaging via NMR spectroscopy. While we will focus on NMR spectroscopy, both techniques require strong expensive magnets and are limited to sample sizes larger than the micron scale. To overcome these requirements and limitations we propose nanoscale zero- to ultralow-field (ZULF) NMR [1,2]. To achieve the goal of nanoscale ZULF NMR, we, together with our collaborators, demonstrated a technique for magnetometry with NV centers in the ZULF regime [3,4] (i.e. Zeeman interaction weaker than j-couplings) Moreover, we are exploring different potential samples and have identified some promising candidates.

Reference

[1] J. W. Blanchard, D. Budker, and Andreas Trabesinger, Lower than low: Perspectives on zero-to ultralow-field nuclear magnetic resonance, *Journal of Magnetic Resonance,* **323**, 106886 (2021) 1
[2] D. Budker, Extreme nuclear magnetic resonance: Zero field, single spins, dark matter. . . , *Journal of Magnetic Resonance,* **306**, Pages 66-68 (2019)
[3] H. Zheng, J. Xu, G. Z. Iwata, T. Lenz, J. Michl, B. Yavkin, K. Nakamura, H. Sumiya, T. Ohshima, J. Isoya, J. Wrachtrup, A. Wickenbrock, and D. Budker, Zero-Field Magnetometry Based on Nitrogen-Vacancy Ensembles in Diamond, *Phys. Rev. Applied,* **11**, 064068 (2019)
[4] T. Lenz, A. Wickenbrock, F. Jelezko, G. Balasubramanian, and D. Budker, Magnetic sensing at zero field with a single nitrogen-vacancy center, *Quantum Science and Technology*, **6**, 3 (2021)

Dipole-dipole interaction between NV$^-$ centers

Chikara Shinei[1], Yuta Masuyama[2], Masashi Miyakawa[1], Hiroshi Abe[2], Shuya Ishii[2], Seiichi Saiki[2], Shinobu Onoda[2], Takashi Taniguchi[1], Takeshi Ohshima[2] and Tokuyuki Teraji[1]

[1] National Institute for Materials Science

[2] National Institutes for Quantum Science and Technology

SHINEI.Chikara@nims.go.jp

Introduction

Negatively charged nitrogen vacancy center (NV$^-$) ensemble with S=1 is a promising color center for highly sensitive magnetometers.[1] Dipole-dipole interaction (DDI) between the NV$^-$ center and paramagnetic defect is one of decoherence mechanisms. In recent study, some studies showed the interaction between the NV$^-$ center and neutral substitutional nitrogen (N_s^0) with S=1/2. The strength of DDI is usually expressed as the multiple of DDI coefficient and concentration of paramagnetic defect. DDI coefficient of N_s^0: $D_{N_S^0}$ is reported as 11.2 ms^{-1} ppm^{-1}.[1] For increasing the NV sensing sensitivity, increasing of [NV$^-$] is needed. Strength of dipole-dipole interaction between NV$^-$ centers is expected to be strong in increasing of [NV$^-$]. The effect of interaction on coherence time T_2 of NV$^-$ center is expected[1] but is not still clear.

In this study, we investigated DDI coefficient of the NV$^-$ center. The DDI coefficient of the NV$^-$ center was evaluated using diamond single crystals with substantial amounts of NV$^-$ center being comparable to that of N_S^0.

Method

Nitrogen doped diamond single crystals used in this study were grown using either HPHT synthesis or CVD method. After the diamond growth, electron beam irradiation was applied with the total fluences of 10^{17}-10^{18} e/cm^{-2} to create vacancies in the diamond. it was followed by vacuum annealing at 1000°C for 2h to form NV centers in the diamond crystals. Concentration of defects and T_2 are evaluated by EPR and Han echo method, respectively.

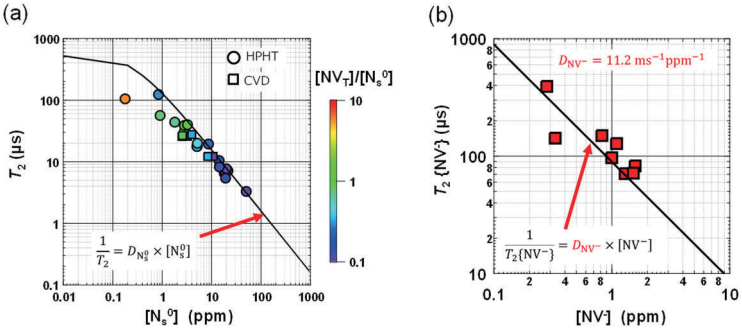

FIG. 1. (a) Relationship between T_2 and concentration of N_s^0. (b) Relationship between T_2 {NV$^-$} and concentration of NV$^-$.

Result and Discussion

First, we investigated dependence of [N_s^0] on T_2 of ensemble of NV$^-$ center. Fig. 1(a) shows relationship between T_2 and [N_s^0]. Most of the data indicates good inverse proportionality between T_2 and [N_s^0], with some exceptional data shown with some deviation from solid line indicating. A larger ratio of [NV_T] to [N_s^0] would be associated with a tendency to greater deviation. This result shows that the decoherence contribution of the spin bath of NV$^-$ and NV^0 centers to the NV$^-$ center spin of interest cannot be ignored. Second, we observe D_{NV^-} center using the data with relatively large [NV_T]/[N_s^0]. We also obtained NV$^-$ component of T_2: T_2{NV$^-$} using equation below,

$$\frac{1}{T_2\{NV^-\}} = D_{NV^-} \times [NV^-] = \frac{1}{T_2} - \{D_{N_S^0}([N_S^0] + [NV^0])\}.$$

Fig. 1(b) portrays relationship between T_2{NV$^-$} and [NV$^-$]. The solid line represents the fitting function curve ($\frac{1}{T_2\{NV^-\}} = D_{NV^-} \times [NV^-]$) with respect to plotting data. We obtained D_{NV^-} of 11.2 ms^{-1} ppm^{-1} through data fitting. This value is nearly equal to that of D_{NV^-} of 10 ms^{-1} ppm^{-1} estimated using the relation between DDI coefficient and spin multiplicity.[1] We observed DDI between NV$^-$ centers with [NV$^-$] ranging from 0.2 ppm to 2 ppm.

Summary

We observed good inverse proportionality between T_2{NV$^-$} and [NV$^-$]. This observation indicates that DDI between NV$^-$ centers occurs with [NV$^-$] ranging from 0.2 ppm to 2 ppm.

Reference

[1] J. F. Barry, J. M. Schloss, E. Bauch, M. J. Turner, C. A. Hart, L. M. Pham, and R. L. Walsworth, Rev. Mod. Phys. **92**, 015004 (2020).

Acknowledgement

This work was supported by MEXT Q-LEAP (JPMXS0118068379 and JPMXS0118067395). T. Teraji acknowledges the support of JST CREST (JPMJCR1773), MIC R&D for construction of a global quantum cryptography network (JPMI00316), and JSPS KAKENHI (Nos. 20H02187, 20H05661 and 19H02617). T. Teraji and S. Onoda acknowledge the support of JST Moonshot R&D (JPMJMS2062).

Extension of dephasing time of ensemble NV centers with a continuous-excitation protocol

Ikuya Fujisaki[1], Yuta Araki[1], Yuji Hatano[1], Takeharu Sekiguchi[1], Takayuki Shibata[2], Takayuki Iwasaki[1] and Mutsuko Hatano[1]

[1]*Department of Electrical and Electronics Engineering, School of Engineering, Tokyo Institute of Technology*

[2]*DENSO Corporation*

fujisaki.i.aa@m.titech.ac.jp

Introduction

Quantum magnetic sensors based on nitrogen-vacancy (NV) centers in diamond are expected to be applied to biological and chemical applications with its high sensitivity. However, the DC magnetic field sensitivity of NV centers is still insufficient for further applications such as magnetoencephalography (MEG). We focused on CE-Ramsey[1] (Continuous Excitation Ramsey), which is not only advantages for miniaturization thanks to its experimental simplicity, but also has high sensitivity compared to conventional Ramsey. CE-Ramsey has a technical issue of long overhead time due to low laser power limited to suppress optical broadening. Dephasing time T_2^* is a key parameter to improve sensitivity, but T_2^* of typical bulk diamond is limited due to high nitrogen density. In this work, we developed a protocol that combines CE-Ramsey with double quantum (DQ) coherence and spin bath driving (SBD)[2] and demonstrated that dephasing time can be extended in the CE protocol.

Methods

We built a compact sensor-head with a CPC lens. Radio frequency system and microwave system are established to manipulate spin bath and NV centers (Fig.1 (a)). We compared dephasing time between CE-SQ-Ramsey and CE-DQ-Ramsey, with and without SBD. The diamond sample ($[NV^-] \sim 0.8$ ppm, $[N_S^0] \sim 8$ ppm) was obtained by electron irradiation (5×10^{17} cm^{-2}) and vacuum annealing (2 hours) after CVD growth (110 um thick) with ^{12}C-enriched methane on a type-IIa substrate.

Results and discussions

We first confirmed coherent control of P1 centers in the spin bath under CE protocol by measuring their spectra and their Rabi oscillations (Fig.1 (b)) with CE-DEER (Double Electron-Electron Resonance) sequences based on the CE-Hahn-Echo. We applied SBD to CE-DQ-4-Ramsey and compared dephasing time. The results showed that the dephasing time is about 2-fold improved by applying DQ and SBD (Fig.1 (c)).

Acknowledgement

This work was supported by MEXT Q-LEAP Grant Number JPMXS0118067395.

We thank Dr. H. Kato (AIST) and Dr. S. Onoda, Dr. T. Ohshima (QST) for supplying diamond samples.

Reference

1. C. Zhang *et al.*, Phys. Rev. Appl. **15**, 1 (2021).
2. E. Bauch *et al.*, Phys. Rev. X **8**, 31025 (2018).

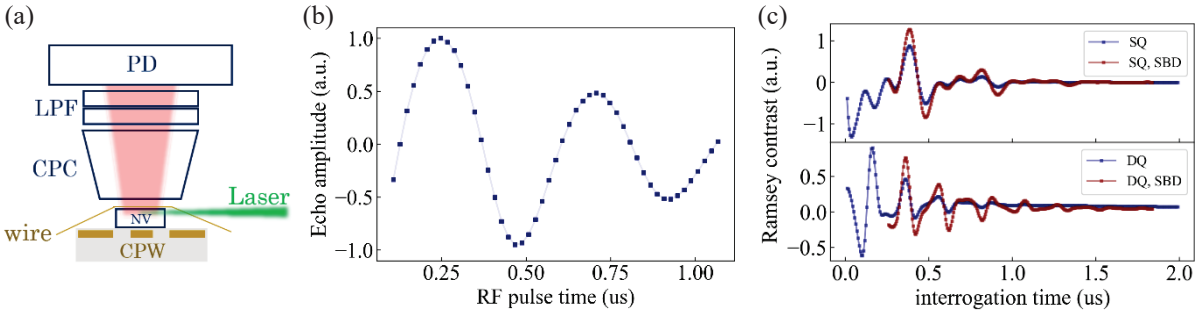

Fig.1. (a) Experimental setup. Microwave and radio frequency are applied with wire and CPW(Coplanar wave guide) respectively. (b) CE-P1 Rabi shows that coherent control of spin bath with CE protocol. Pulse time of RF (radio frequency) is swept in CE-DEER sequences. (c) 2-fold extension of dephasing time by applying DQ and SBD to CE-Ramsey.

SE-03A-β1-02

Wide temperature operation of diamond quantum sensor for electric vehicle battery monitoring

Keisuke Kubota[1], Yuji Hatano[1], Yuta Kainuma[1], Daisuke Nishitani[1], Takashi Taniguchi[2], Tokuyuki Teraji[2], Shinobu Onoda[3], Takeshi Ohshima[3], Takayuki Iwasaki[1], and Mutsuko Hatano[1,3]

[1]*Department of Electrical and Electronic Engineering, School of Engineering, Tokyo institute of technology, 2-12-1 Ookayama, Meguro, Tokyo 152-8552, Japan*

[2]*National Institute for Materials Science, 1-1 Namiki, Tsukuba, Ibaraki 305-0044, Japan*

[3]*National Institutes for Quantum Science and Technology, 1233 Watanuki-machi, Takasaki, Gunma 370-1292, Japan*

kubota.k.ai@m.titech.ac.jp

Introduction

The diamond quantum sensors containing NV centers for electric vehicle(EV) battery monitoring are realized [1]. Sensors for EV batteries require a wide range of operating temperatures; however, the dependence of the sensitivity of the diamond quantum sensor system on its wide operating temperature has not been reported. Therefore, we measured the magnetic field sensitivity in the temperature range from -150° to 150°C to investigate its potential for battery monitoring.

Methods

The overall configuration of the measurement system used in the experiment, including the sensor head, is shown in Fig.1 (a). The diamond sensor was a (111) HPHT crystal with the size of approximately 3.6 mm^3. 1×10^{18} electrons/cm^2 electron beam irradiation and 1000 ℃ for 1 hour annealing after it realized 5 ppm NV density. The diamond sensor was attached to the top of the multimode fiber and the surrounding microwave antenna with copper belt was attached to realize the sensor head with a size of $1 \times 1 \times 0.5$ cm^3. The green excitation light from the fiber, with an intensity of approximately 200 mW at the end of the fiber, was irradiated to the diamond sensor. Liquid nitrogen and a heater were used to vary the temperature.

Result and discussion

Fig.1 (b) shows the temperature dependence of the measured sensitivity of the magnetic field. The sensitivity of approximately 5 $nT/Hz^{1/2}$ was confirmed in the temperature range of -150–150 °C in the measurement system at atmospheric pressure as shown in Fig.1 (a). This sensitivity means that 10 mA current can be measured almost in 500 Hz bandwidth in the temperature range between -150 and 150 °C. The confirmed current sensitivity in such a wide temperature range makes it suitable for the batteries that are currently used or under development. Fig.1 (c) shows the temperature dependence of the shot noise sensitivity obtained from the contrast, line width, and photodiode (PD) current. On the high temperature side, as we had expected, the sensitivity deteriorated with increasing temperature. This deterioration is mainly due to the contrast deterioration, which can be attributed to the accelerated initialization of the spin state due to the faster singlet state transition rate [2]. On the low temperature side, we had expected that the sensitivity would be improved, but it deteriorated. Deterioration in contrast was the main cause, but it is difficult to explain the physical reasons. Considering that the line width is thinner at lower temperatures, water vapor condensation at microwave antenna may have increased antenna loss because this experimental setup was open to the atmosphere.

This work was supported by MEXT Quantum Leap Flagship Program (Q-LEAP) Grant Number JPMXS 0118067395 and JPMXS0118068379.

References

[1] Y. Hatano et al., Sci. Rep. 12, 13991 (2022)

[2] D. Toyli et al., Phys. Rev. X 2, 031001 (2012)

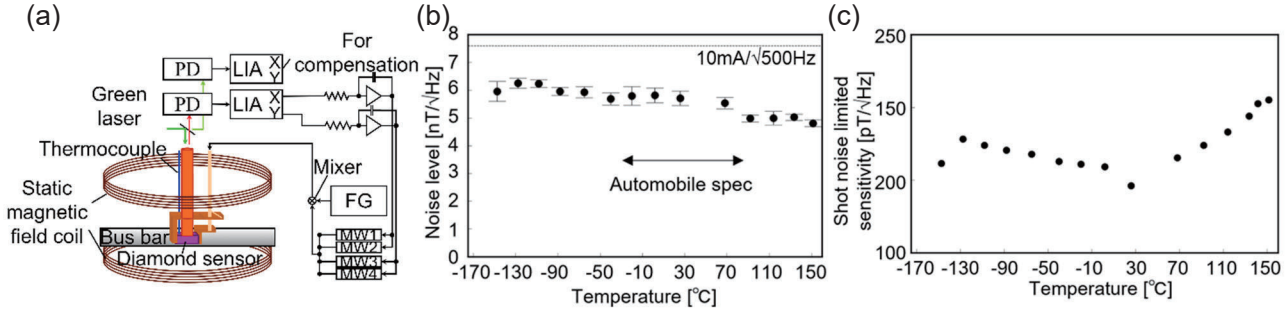

Fig.1 (a) Structure of the entire sensitivity measurement system. The dimension of the sensor head was approximately 1 × 1 × 0.5 cm^3. (b) Temperature dependence of the measured sensitivity. It was confirmed that the current sensitivity requirements for EV batteries were obtained in the measured temperature range. (c) Measured temperature dependence of shot noise sensitivity obtained from contrast, line width, and PD current.

A development of wearable magnetic shield for MEG

Soichiro Shido[1], Masato Hasegawa[2], Motofumi Fushimi[1], Shinichi Chikaki[1], Masaki Sekino[1]
[1]Department of Bioengineering, School of Engineering, The University of Tokyo
[2]Department of Electrical Engineering and Information Systems, School of Engineering, The University of Tokyo
shido-soichiro@g.ecc.u-tokyo.ac.jp

Introduction

MEG is a technique for measuring the magnetic field generated by the electrical activity of neurons. The brain's magnetic field is about 100fT, which is very small, about 1/100 million of the geomagnetic field. MEG is currently used primarily for the diagnosis of epilepsy[1]. MEG has a high potential to become brain imaging technology.

However, the current MEG is limited with superconducting quantum interference devices (SQUIDs) [2]. Vacuum space of SQUID makes it difficult to use closer than ~2 cm to the scalp. That was one of the problems. Recently, new sensor-enabled construction of wearable MEG systems. Optically pumped. magnetometers (OPM) have made it possible.

One of the great missions of operating MEG is controlling the magnetic field. MEG systems have magnetic shield rooms (MSR). Originally they have mainly two types of shields. multiple layers of high magnetic permeability metal (e.g. mu-metal) to exclude low-frequency (DC to ~10 Hz) magnetic fields, and a layer of metal with a high electrical conductivity (such as copper or aluminum) to attenuate higher-frequency (>10 Hz) magnetic fields[2]. However, thanks to wearable sensors (OPM**,** **NV**) MEG systems are getting more wearable with the movement of participants. These MSRs often result in a 'remnant' DC magnetic field. So, OPMs are built with electromagnetic coils. (Fig.1) is the outlook of a typical system. Compared to the system, we propose a wearable shield system (Fig.2).

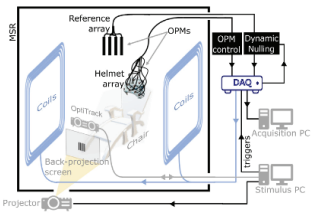

FIG. 1. Typical OPM-MEG system[4]

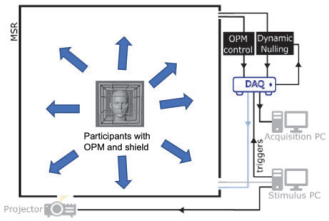

FIG. 2. Our proposal system[4]

In this system, participants can move freely inside the MSR. With this system, we can give participants a comfortable experience of MEG. For the building of the shield, the major steps were the design of the helmet (Fig.3), the optimal design of the coils with target field method (Fig.4), the design of the control system(Fig.5), and the design of the circuit.

In this control system, we applied a PI control system, and the purpose value of this system is to attenuate the Magnetic field into 2nT which is the typical ability of shields with electromagnetic coils. For the circuit, Gradient magnetic field circuit is used. With this circuit, only the ratio of voltage and resistor changes the current of the circuit. So, it is easy and simple to control. To simulate the ability of this shield, we compared designed coil and the Merritt coil which is one of the coils generate uniform magnetic shields. In particular, the magnetic field was not uniform at the bottom of the shield. This may be due to the asymmetry of the shape of the head from front to back. Therefore, it is necessary to consider various improvement plans, such as design changes that take this shape into account and control methods that do not require a uniform magnetic field for the entire helmet.

FIG. 3. The helmet designed in this research

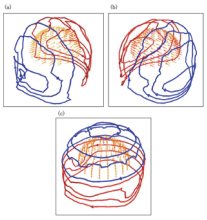

FIG. 4. Coils designed in this research

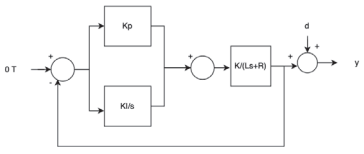

FIG. 5. Control system of this shield

Acknowledgement

This work was supported by MEXT Q-LEAP Grant Number JPMXS0118067395.

Reference

1 Baker, Elife,3, e01867(2014).
2 Cohen, Science,161,664-666(1972).
3 Hoburg, IEEE Transactions on Electromagnetic Compatibility,37,574-579(1995).
4 M Rea, NeuroImage,241,118401(2021).

Attempts to generate entanglement state between dipolar coupled NV centers created by molecular implantation

Kosuke Kimura[1,2], Shinobu Onoda[1], Keisuke Yamada[1], Wataru Kada[2], Tokuyuki Teraji [3], Junichi Isoya[4], Nozomu Kosuge[1,2], Tomoya Baba[1,2], Osamu Hanaizumi[2], and Takeshi Ohshima[1]

[1] *National Institutes for Quantum Science and Technology*

[2] *Graduate School of Science and Technology, Gunma University*

[3] *National Institute for Materials Science*

[4] *Faculty of Pure and Applied Sciences, University of Tsukuba*

kimura.kosuke@qst.go.jp, *t222d002@gunma-u.ac.jp.*

Introduction

Generating quantum entanglement states is one of the most important steps in quantum technologies such as quantum information processing and quantum sensing, etc. The generation of entanglement states has been demonstrated on the various quantum systems. Among them, the entanglement between some solid-state spin qubits has the generation advantage at room temperature. Generation of entanglement state between Nitrogen-Vacancy (NV) centers in diamond, known as solid-state electron spin qubits, has been demonstrated by Double Electron-Electron Resonance (DEER)[1,2]. The decoherence of NV center limits the fidelity of entanglement state. It is expected that the short free evolution time for entanglement ($2\tau_{ent}$) reduce the limitations caused by decoherence. The spin state reaches the maximum quantum entanglement state at the free evolution time $2\tau_{ent} = 1/\upsilon_{dip}$ by DEER, where υ_{dip} is dipole coupling strength. By making the dipole-dipole interaction as strong as possible, high fidelity due to short free evolution time is expected. We have created the strongly coupled NV centers by molecular ion implantation[3,4]. In this study, we report the generation of entanglement state between dipolar coupled double NV centers created by implanting $C_5N_4H_n$ ions. In addition, we report the attempts to shorten $2\tau_{ent}$ by changing DEER pulse sequence.

Experiments and Results

To create dipolar coupled NV centers, $C_5N_4H_n$ ions were accelerated at 65 keV and implanted into diamond. A $C_5N_4H_n$ ion decomposes into individual atoms by collision with diamond, and each nitrogen atom is implanted 9±4 nm apart. The implanted nitrogen atom was combined with a vacancy by annealing process (1000°C, 2h) to create NV centers.

The created NV centers were observed using confocal fluorescence microscopy (CFM). The measurement of DEER was performed with a 532 nm pulsed laser and pulsed microwaves at room temperature in the static magnetic field (FIG. 1). The electron spins of two NV centers with different resonance frequencies (2.6279 GHz for NV_A, 2.6778 GHz for NV_B) able to be manipulated individually. Preparing both NV centers in state $|m_{S,A} = 0, m_{S,B} = 0\rangle$ by optical pumping, an echo measurement is carried out on NV_A. To apply π/2 pulse on NV_B before the second π/2 on NV_A, fluorescence is a periodical signal of $cos(2\pi\upsilon_{dip}\tau)$. The result of the DEER measurement is shown in FIG. 2. The measured υ_{dip} was 99.9 kHz and $2\tau_{ent} = 1/\upsilon_{dip}$ was calculated as 10 μs. In the presentation, the entanglement generation with other pulse sequences will be discussed.

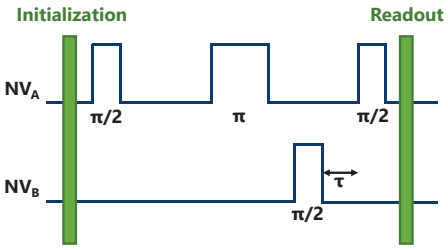

FIG. 1 DEER pulse sequence.

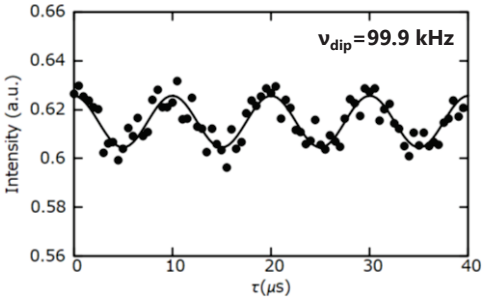

FIG. 2 Typical DEER spectrum.

Acknowledgments

This work was supported by JST Support for Pioneering Research Initiated by the Next Generation JPMJSP2146, JSPS KAKENHI No. 21H04646, 20H02187, 20H05661, JST moonshot R&D Grant Number JPMJMS2062, MIC R&D for construction of a global quantum cryptography network JPMI00316, and MEXT Quantum Leap Flagship Program (MEXT Q-LEAP) Grant Number JPMXS0118067395 and JPMXS0118068379.

References

[1] P. Neumann, *et al.*, Nat. Phys. **6**, 249 (2010). [2] F. Dolde, *et al.*, Nat. Phys. **9**, 139 (2013).
[3] M. Haruyama, *et al.*, Nat. Commun. **10**, 2664 (2019). [4] K. Kimura, *et al.*, Appl. Phys. Express **15**, 066501 (2022).

Charge stability of shallow single NV centers in p-type diamond

Taisuke Kageura[1,2], Yosuke Sasama[1], Chikara Shinei[1], Tokuyuki Teraji[1], Keisuke Yamada[3], Shinobu Onoda[3], and Yamaguchi Takahide[1]
[1]*National Institute for Materials Science (NIMS)*
[2]*National Institute of Advanced Industrial Science and Technology (AIST)*
[3]*National Institutes for Quantum and Radiological Science and Technology (QST)*
kageura.taisuke@aist.go.jp

Introduction

A stable negatively charged state of nitrogen vacancy (NV) centers in diamond is important for diamond quantum applications such as highly sensitive quantum sensing and high-performance quantum information processing. However, it has been found that the charge state of single NV centers near the surface, called shallow single NV centers, is quite unstable compared with NV centers in bulk[1]. Shallow single NV centers are significant to realize high-performance quantum devices such as nanoscale NMR, so the origin of the charge instability needs to be revealed. Here we investigated how the presence of small amounts of boron acceptors in bulk and surface states affect the charge stability of shallow single NV centers[2].

Results and Discussion

We prepared four lightly boron-doped diamond thin films ([B]≤1×10^{15} cm^{-3}, [N]<6×10^{11} cm^{-3}) synthesized by microwave plasma chemical vapor deposition method and formed single NV centers at about 3.6 nm from the diamond surface by ion implantation. We have investigated the charge-state stability of the shallow single NV centers by using photoluminescence spectra and optically detected magnetic resonance (ODMR) measurements. Surprisingly, we found that negatively charged state can be created despite the existence of boron acceptors; Among 20 NV centers for which CW-ODMR was measured, 19 NV centers showed a decrease in fluorescence intensity at a frequency corresponding to the applied magnetic field of 1-2 mT. This negatively charged state could not be explained by the conventional band-bending model, but it could be explained by photoexcitation induced by green laser irradiation. Then we evaluated the charge stability under pulse measurement in the presence of laser non-irradiation time by Rabi oscillation contrast values (Fig. 1). Clear Rabi oscillations were observed except for the sample with higher boron concentration ([B]=1×10^{15} cm^{-3}) and acid boiled surface, which means that negatively charged state can be created even under pulse measurement. The variation of contrast values in Fig. 1(b) indicates the difference in charge stability of individual NV centers. This charge instability in lightly doped diamond can be explained by electron transfer between the NV center and the local environment. The charge stability is determined by whether the donor or the acceptor is closer to the NV center.

This study provides a new insight into the charge stability of a single NV center in low-doped diamond and contributes to the further development of NV quantum devices.

This work was partially supported by MEXT Q-LEAP Grant Number JPMXS0118068379 and JPMXS0118067395, JST CREST (JPMJCR1773), JST Moonshot R&D (JPMJMS2062), MIC R&D for construction of a global quantum cryptography network (JPMI00316), JSPS KAKENHI (No. 20H02187, 20H05661, 19H02617 and 21J01804).

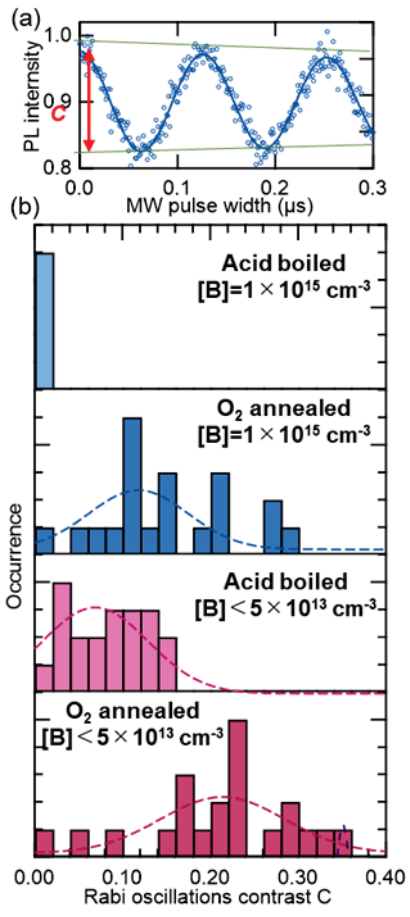

FIG. 1. (a) Typically observed Rabi oscillations and (b) the distributions of Rabi contrast

Reference

[1] D. Bluvstein et al., *Physical Review Letters*, 122, 076101 (2019)
[2] T, Kageura et. al, *Carbon*, 192, 473 (2022).

Room-temperature electrical detection of nuclear spins in silicon carbide

Naoya Morioka[1,2], Tetsuri Nishikawa[1], Hiroshi Abe[3], Hiroki Morishita[1,2], Takeshi Ohshima[3], and Norikazu Mizuochi[1,2]
[1] *Institute for Chemical Research, Kyoto University*
[2] *Center for Spintronics Research Network, Institute for Chemical Research, Kyoto University*
[3] *National Institutes for Quantum Science and Technology*
morioka.naoya.8j@kyoto-u.ac.jp

Spin-active color centers in silicon carbide (SiC) are promising candidates for scalable quantum sensors and quantum information devices operating at room temperature due to their excellent spin coherence properties and the maturity of SiC's wafer-scale semiconductor technology. By making use of the excellent controllability of semiconductor properties and device operation of SiC, the realization of electrical detection of spin information in SiC can benefit in developing integrated quantum devices compared with conventional optical spin detection techniques. Recently, electrical detection of electron spins of the V2 center in 4H-SiC[1] was reported by photoelectrically detected magnetic resonance[2] (PDMR). However, in the previous demonstration, the PDMR spectra of V2 centers were broad due to the inhomogeneous magnetic field caused by magnetized Ni electrodes, which is a typical ohmic contact material for SiC. The broad linewidth inhibited resolving the signal of nuclear spins, which are useful resources as quantum memories for quantum information processing[3] and sensitivity-enhanced quantum sensing.[4] In this study, we optimized the contact and the device structures, and we obtained the PDMR spectrum of an ensemble of V2 centers with a linewidth of 2.8 MHz, which is narrow enough to observe the hyperfine split resonance peaks coupled to the next-nearest-neighbor (NNN) ^{29}Si nuclear spins (Fig. 1). By addressing the hyperfine split peaks, nuclear-spin-state-dependent spin control and its electrical detection are possible. By applying these techniques, the nuclear magnetic resonance signal of ^{29}Si was successfully detected electrically at room temperature with PDMR-based electron-nuclear double resonance (ENDOR) (Fig. 2).[5] This is an achievement of electron spin coherence and nuclear spin detection in an identical device. In the ENDOR spectrum in Fig. 2, three peaks were observed, probably originating from three nonequivalent NNN sites.[6] These results suggest that room-temperature PDMR would enable selective coherent control of nuclear spins, facilitating the development of electrically-driven integrated quantum devices.

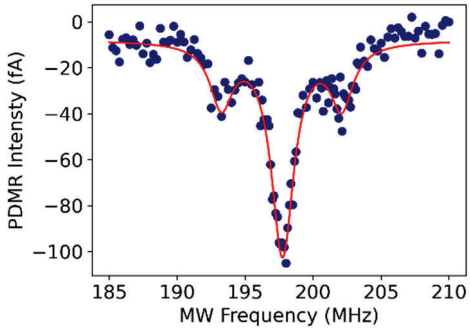

FIG. 1. PDMR spectrum of V2 centers in 4H-SiC.

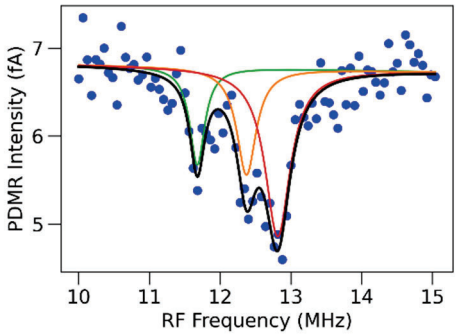

FIG. 2. PDMR-ENDOR spectrum of NNN ^{29}Si nuclear spins coupled to V2 centers in 4H-SiC.

Acknowledgments

This work was supported by MEXT Q-LEAP Grant Number JPMXS0118067395, JSPS KAKENHI Grant Numbers JP20H00355, JP21H04553, JP21K20502, and JP22H01526, JST SPRING Grant Number JPMJSP2110, and Kyoto University Nanotechnology Hub in MEXT ARIM project.

Reference

[1]M. Niethammer et al., Nat. Commun., 10, 5569 (2019).
[2]E. Bourgeois et al., Nat. Commun., 6, 8577 (2015).
[3]C. E. Bradley et al., Phys. Rev. X, 9, 031045 (2019).
[4]M. Pfender et al., Nat. Commun., 10, 594 (2019).
[5]T. Nishikawa et al., Appl. Phys. Lett., accepted (2022).
[6]V. Ivády et al., Phys. Rev. B, 96, 161114 (2017).

(Near) zero-field cross-relaxation features for ensembles of NV centers in diamond

Omkar Dhungel[1], Till Lenz[1], and Dmitry Budker[1,2]

[1]*Johannes Gutenberg University Mainz, Germany*

Helmholtz Institute Mainz 55128, Germany

[2]*Department of Physics, University of California, Berkeley, California 94720-300, USA*

budker.uni-mainz.de

Conventional magnetometry using NV centers in diamond relies on the application of microwaves and bias magnetic field. However, there are applications, for example, the study of high-temperature superconductors, zero- to ultralow-field (ZULF) NMR, investigation of biological samples, and magnetic materials where either the microwaves or the bias magnetic field might disturb the system. To overcome such limitations, we study the zero-field cross-relaxation feature [1] for ensembles of NV centers. A study of cross-relaxation features with respect to the sample cut and, NV density will be presented. Multiple cross-relaxation features [2,3] are observed when transverse field is present and these features follow a specific pattern when the azimuthal angle of a transverse field is changed, which is useful for vector-magnetometry applications.

Reference

[1]S. Anishchik, V. Vins, A. Yelisseyev, N. Lukzen, N. Lavrik, and V. Bagryansky, "Low-field feature in the magnetic spectra of nv- centers in diamond," New Journal of Physics, vol. 17, no. 2, p. 023040, 2015.

[2]R. Akhmedzhanov, L. Gushchin, N. Nizov, V. Nizov, D. Sobgayda, I. Zelensky, and P. Hemmer, "Microwave-free magnetometry based on cross-relaxation resonances in diamond nitrogen-vacancy centers," Physical Review A, vol. 96, no. 1, p. 013806, 2017.

[3]R. Akhmedzhanov, L. Gushchin, N. Nizov, V. Nizov, D. Sobgayda, I. Zelensky, and H. Philip, "Magnetometry by cross-relaxation-resonance detection in ensembles of nitrogen-vacancy centers," Phys. Rev. A, vol. 100, p. 043844, Oct 2019.

Evaluation of a superconducting nanowire single photon detector for mid-infrared wavelengths

Satoru Mima [1], Fumihiro China [1], Masahiro Yabuno [1], Shigeyuki Miyajima [1], Shigehito Miki [1, 2], Yuki Gama [3], Toshiyuki Tashima [3], Masaya Arahata [3], Yu Mukai [3], Ryo Okamoto [3], Shigeki Takeuchi [3] , Hirotaka Terai [1]

[1] *Advanced ICT Research Institute, National Institute of Information and Communications Technology*

[2]*Graduate School of Engineering, Kobe University*

[3]*Graduate School of Engineering, Kyoto University*

mima@nict.go.jp

Introduction

Superconducting nanowire single photon detectors (SNSPDs) have attractive features such as high efficiency, low jitter, low dark counts, and high counts rates, and are expected to be applied in various fields. Recently, quantum technologies utilizing photons in the mid-infrared region have attracted much attention[1]. However, there are no single-photon detectors in the mid-infrared wavelengths. SNSPD is one of best candidate for high detection efficiency in the mid-infrared region.

In the mid-infrared region, the photon energy is smaller than in the near-infrared region, so the superconducting thin film used in the detector must be thinner and superconducting nanowire must be narrower. In addition, for highly efficient mid-infrared photon detection, the introduced light must be efficiently absorbed by the superconducting nanowire. We employ an approach to enhancing the optical absorptance at target wavelength is integrating the nanowire with the dielectric multilayer cavity[2]. In this study, superconducting nanowire were fabricated on a dielectric multilayer of Ta_2O_5 and Si films designed to maximize light absorption in the mid-infrared region and evaluated.

We cooled down the fabricated detector by a sorption refrigerator capable of cooling down to 0.8 K and evaluate the optical properties using a QCL light source (wavelength ~ 4.3 μm) in the mid-infrared region. We reduced optical efficiency between the fiber and the superconducting nanowire for the evaluation of internal efficiency because of the intensity of blackbody radiation in the mid-infrared region. The figure 1 shows the dependence of the internal efficiency of the superconducting nanowire on the bias current measured at different intensities of the mid-infrared light source. We also evaluated the optical efficiency of the same superconducting nanowire in the near-infrared region (1300 nm to 1600 nm) and confirmed that the spectra are consistent with the design.

Acknowledgment

This work was supported by MEXT Q-LEAP Grant Number JPMXS0118067634.

Reference

[1]R. H. Hadfield, *Nat. Photon.*, 3, 696–705 (2009).
[2]T. Yamashita, K. Waki, S. Miki, R. A. Kirkwood, R. H. Hadfield, H. Terai, *Sci rep.*, 6, 35240 (2016).

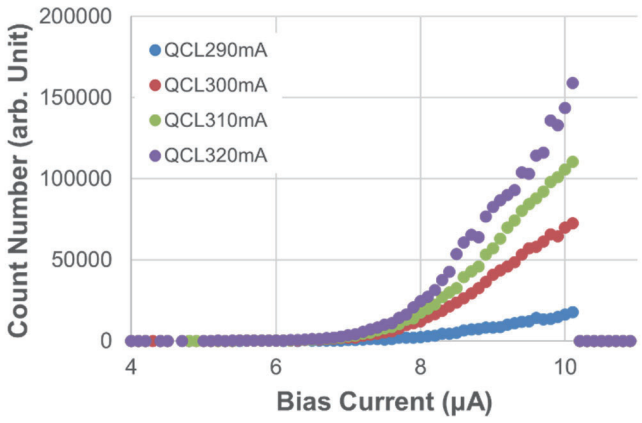

Fig 1. Comparison of the intensity dependence of the internal efficiency in the mid-infrared.

Efficient superconducting nanostrip single-photon detectors for 2 μm wavelength

Fumihiro China[1], Satoru Mima[1], Shigehito Miki[1,2], Masahiro Yabuno[1], Shigeyuki Miyajima[1] and Hirotaka Terai[1]

[1] *Advanced ICT Research Institute, National Institute of Information and Communications Technology*

[2] *Graduate School of Engineering, Kobe University*

f-china@nict.go.jp

Introduction

In recent years, single-photon detection technology in the mid-infrared wavelength region has attracted attention. In particular, at the 2 μm wavelength band, highly efficient single-photon detectors are required for various applications such as light detection and ranging (LIDAR), satellite-based quantum communications, and silicon-based quantum optics. However, semiconductor avalanche photodiodes and photomultiplier tubes are limited to a sensitive wavelength of approximately 1.8 μm by the energy gap of the semiconductor. On the other hand, superconducting nanostrip single-photon detectors (SNSPDs) are promising detectors because of their wideband sensitivity including the mid-infrared region [1]. To obtain high system detection efficiency (SDE) using SNSPDs, the following three factors should be maximized: optical coupling efficiency, optical absorptance, and internal detection efficiency. The optical coupling efficiency can be maximized by increasing the active area of the SNSPD, and the optical absorptance of superconducting nanostrips is improved by implementing an optical cavity in the SNSPD. The internal detection efficiency can be improved by optimizing nanostrip parameters such as nanostrip width and thickness. In this study, we developed SNSPDs with a dielectric multilayer cavity (DMC) and attempted to maximize the three factors to achieve high SDE in the 2 μm wavelength.

Device design and experimental results

We developed NbTiN-SNSPDs with a DMC. Figure 1 shows the schematic of designed SNSPDs with a DMC comprised of 11 periodic SiO_2/Si bilayers on a Si wafer. Each dielectric layer of DMC is one-quarter of the optical thickness for the 2 μm wavelength. The DMC enhances the optical absorptance by concentrating the electric field of incident photons on the nanostrips. In the simulation results by finite element analysis, we confirmed that the optical absorptance at the 2 μm wavelength reaches over 99%. Based on the SNSPD designs, we fabricated NbTiN-nanostrips with a line width of approximately 110 nm on the DMC. The active area of the fabricated SNSPDs, 30 μm × 30 μm, is enough larger than the mode field diameter of a single mode fiber for the 2 μm wavelength band. Subsequently, we tested the fabricated SNSPDs using a sorption-based cryocooler with an operating temperature of 0.77 K and an optical system composed of a laser source, a beam splitter, valuable optical attenuators (VOAs), neutral-density (ND) filters, a polarization controller, and power meters. We adjusted the optical input power to -110 dBm using three VOAs and two ND filters, and all five attenuators were carefully calibrated before SDE measurements. Figure 2 shows the measurement results of SDE and the dark count rate (DCR) of the SNSPD. We succeeded to demonstrate a high SDE of 79% at a 2 μm wavelength. In addition, we estimated the measurement uncertainty of SDE as ±5.075% by measuring all possible uncertainties of VOAs, ND filters, laser power, the count rate, DCR, and a power meter.

Acknowledgment

This work was supported by MEXT Q-LEAP Grant Number JPMXS0118067634.

Reference

[1]F. Marsili et al., *Nano Lett*, 12, 4799-4804 (2012).

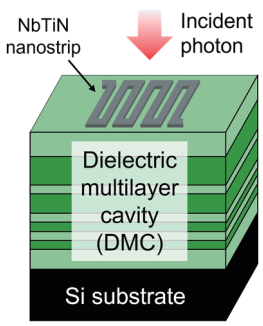

FIG. 1. Schematic of the device structure of an SNSPD with a DML.

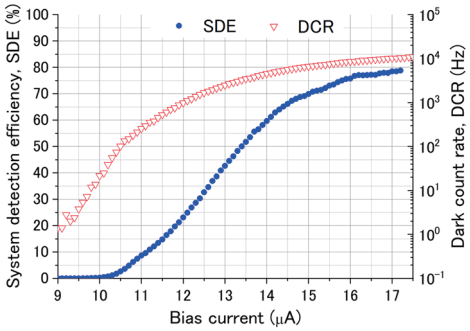

FIG. 2. Bias current dependences of system detection efficiency (SDE) and dark count rate (DCR).

Effect of pump laser linewidth on nonlinear quantum interferometric fringes

Jasleen Kaur[1], Yu Mukai[1], Ryo Okamoto[1] and Shigeki Takeuchi[1*]
[1]*Department of Electronic Science and Engineering, Graduate School of Engineering, Kyoto University*
*takeuchi@kuee.kyoto-u.ac.jp

Introduction

Infrared spectroscopy is a non-invasive technique used for the identification of materials by analyzing their infrared spectrum. This technique finds applications in chemical industries, environmental sensing, and life sciences, etc. However, conventional infrared spectroscopy techniques suffer from low directivity of infrared sources and thermal background noise deteriorating the sensitivity of IR detectors. Therefore, quantum infrared spectroscopy (QIRS) [1] is being widely investigated as this quantum sensing technology enables IR spectroscopy using a light source and detector in the visible region. In this technique, by utilizing the quantum correlation between visible and IR photon pairs and the quantum interference of their generation processes, we can extract the optical properties of the IR absorptive sample.

The generation of correlated photon pairs in QIRS relies on the spontaneous parametric down-conversion (SPDC) process. Since the current QIRS experiments have been demonstrated using a continuous wave (CW) laser [2,3], the probe photon flux generated is low, leading to an inferior signal-to-noise ratio (SNR) thus limiting the sensitivity of this technique. Achieving high generation efficiency of the PDC process can aid in increasing the SNR of the system. One of the possible ways is to use a short pulse pump laser as the excitation source. The temporal confinement of energy in a pulse laser helps in increasing the parametric gain of the PDC process. However, it is important to note that the pulse laser possesses a finite spectral linewidth which leads to a partial frequency correlation between the generated photon pairs, leading to increased distinguishability between the photons, thus lower interference contrast.

In this work, we report a quantitative analysis of how the pump laser linewidth affects the nonlinear quantum interferometer. As shown in fig.1, we excite a nonlinear quantum interferometer with both CW and pulse laser sources and compare the contrast of fringes using a dispersive spectrometer. We further derive the mathematical relationship between the interferometric pattern obtained by CW and pulse laser.

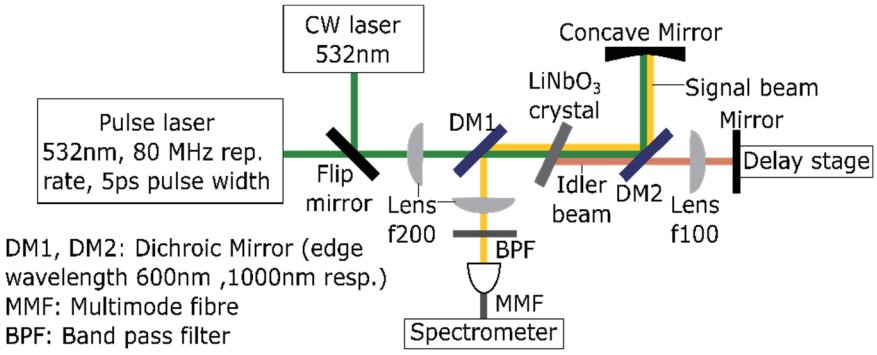

FIG. I. Schematic of the nonlinear quantum interferometer

Reference

[1]D. A. Kalashnikov *et al.* Nat. Photonics, vol. 10, no. 2, p. 98–101 (2016)

[2]Y. Mukai *et al.* Phys. Rev. Appl., vol. 15, no. 3, p. 034019 (2021)

[3]P. Kaufmann *et al.* Opt. Express, vol. 30, no. 4, p. 5926 (2022)

Acknowledgment

This work was supported by MEXT Q-LEAP Grant Number JPMXS0118067634, JST-CREST Grant Number JPMJCR1674, JSPS KAKENHI Grant Number 21H04444, and WISE Program, MEXT

Highly efficient and ultra-broadband photon pair source using chirped quasi-phase matching slab waveguide

Bo Cao[1], Kyohei Hayama[1], Shun Suezawa[1], Mamoru Hisamitsu[2], Katsuhiko Tokuda[2], Sunao Kurimura[3], Ryo Okamoto[1], and Shigeki Takeuchi[1]
[1]*Department of Electronic Science and Engineering, Kyoto University*
[2]*Shimadzu Corporation*
[3]*National Institute for Materials Science (NIMS)*
takeuchi@kuee.kyoto-u.ac.jp

Introduction

Entangled photon pairs with a broad spectral bandwidth are essential components in many quantum optical applications, such as quantum information, quantum communication and quantum sensing. One of the most rapidly developed technologies is quantum optical coherence tomography (QOCT) [1, 2]. To improve the performance for above applications, highly efficient ultra-broadband frequency correlated photon pair sources are required. In a previous work, we reported a demonstration of high efficiency and broadband frequency correlated photon pair collinear generation (photon are emitted into the same spatial mode) using a ridge-waveguide- based chirped quasi-phase matching (QPM) device [3]. However, two photon interference-based applications, like QOCT, cannot directly use collinearly emitted photon pairs. To solve this problem, here we report a scheme using a slab waveguide based chirped QPM device for the generation of highly efficient and ultra-broadband frequency correlated photon pairs under a non-collinear emission (emit photon pairs into separated spatial modes) condition. In experiments, we observed a generation efficiency of 8.2×10^5 pairs/(s·μW) and a spectral bandwidth of 190 nm in full width half maximum (FWHM). In addition, we also used slab waveguides as photon pair sources in the two-photon interference experiments.

Experiments and results

The schematic view of this slab waveguide device is shown in Fig. 1. In this device, a layer of stoichiometric lithium tantalate (SLT) with a thickness of ~3 μm is used as the waveguide core and resin is used as the cladding material. This waveguide is designed for the generation of photons with a central wavelength at 810 nm using 405 nm continuous wave (CW) pump light via a type-0 spontaneous parametric down conversion (SPDC) process.

We first measured the non-collinearly emitted photons spectra after single mode fiber coupling. In the case of using a non-chirped slab waveguide, we observed a spectrum with a bandwidth of 26 nm, and when using a 3% chirped QPM slab device, the spectral bandwidth expended to 190 nm in FWHM. We also carried out a coincidence measurement using two single photon detectors (SPCMs) and time analyzer to estimate the generation efficiency. The generation efficiencies for the non-chirped device and the 3% chirped device are 2.4×10^6 pairs/(s·μW) and 8.2×10^5 pairs/(s·μW) respectively.

Finally, we performed Hong-Ou-Mandel (HOM) measurements using the non-collinearly emitted photon pairs generated from slab waveguides. The interference resulted a HOM dip with an FWHM width of 8.2 μm when using a non-chirped device, and a HOM dip with an FWHM width of 2 μm when using a 3% chirped device.

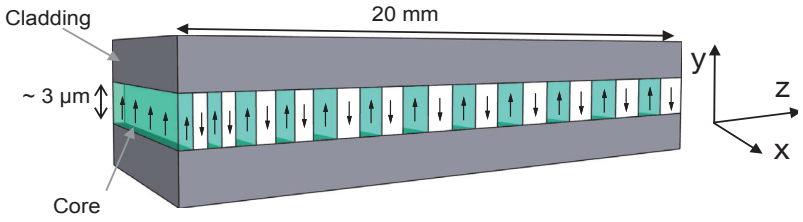

FIG. 1. The schematic view of a slab waveguide device.

This work was supported by JST-CREST (JPMJCR1674), MEXT Quantum Leap Flagship Program (JPMXS0118067634), JSPS KAKENHI (21H04444) and MEXT WISE Program.

Reference

[1]A. F. Abouraddy, M. B. Nasr, B. E. A. Saleh, A. V. Sergienko, and M. C. Teich, Phys. Rev. A 65, 053817 (2002).
[2]K. Hayama, B. Cao, R. Okamoto, S. Suezawa, M. Okano, and S. Takeuchi, Opt. Lett. 47, 4949-4952 (2022).
[3]B. Cao, M. Hisamitsu, K. Tokuda, S. Kurimura, R. Okamoto, and S. Takeuchi, Opt. Express 29, 21615-21628 (2021).

Optical trapping and movement control of gold nanoparticles on an optical nanofiber

Rui Sun[1,2], Yining Xuan[1,2], Soyoung Baek[1], and Keiichi Edamatsu[1]
[1]*Research Institute of Electrical Communication, Tohoku University*
[2] *Department of Electronic Engineering, Graduate School of Engineering, Tohoku University*
sun.rui.p6@dc.tohoku.ac.jp

Introduction

Optical nanofiber has drawn lots of interests in past few years as a promising tool in quantum optics and quantum metrology for its unique properties[1,2]. Our research focus on the single photon source based on quantum-dot-gold-nanoparticle coupled system on optical nanofiber[3]. With this experimental system, we have realized a single photon source which is much better than directly exciting the quantum dot with laser. For instance, significant Purcell enhancement of the single photon emission rate was observed[4].

However, the current experimental system still has some drawbacks. The position of gold-nanoparticle on nanofiber is entirely random, which makes it difficult to quantitatively study the single-photon emission rate. Thus, we propose a non-contact method to control the position of a gold-nanoparticle on the nanofiber. In the past research, we have realized to control the motion of liposome particles in solution by changing the intensity of evanescent light field on the optical nanofiber surface[5]. Here, following a similar approach, we report on a protocol to achieve the control of gold nanoparticles on an optical nanofiber to further improve the properties of single photon source. As shown in Figure 2, the optical nanofiber is immersed in the solution containing gold nanoparticles, and 785 nm laser and 530 nm laser are injected at both ends of the nanofiber respectively. 785 nm laser is used to generate evanescent light field, and 530 nm laser is used to detect the movement of the gold nanoparticles on the surface of optical nanofiber. By adjusting the laser intensity, we can control the movement of the gold nanoparticles on the nanofiber surface. We will introduce optical tweezer to this system to achieve more precise position control of gold nanoparticles.

This work is supported by MEXT Q-LEAP Grant Number JPMXS0118067581.

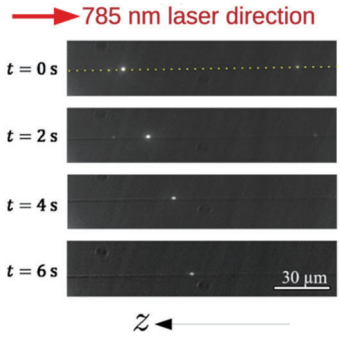

FIG. 1. The movement of a liposome along the nanofiber[5].

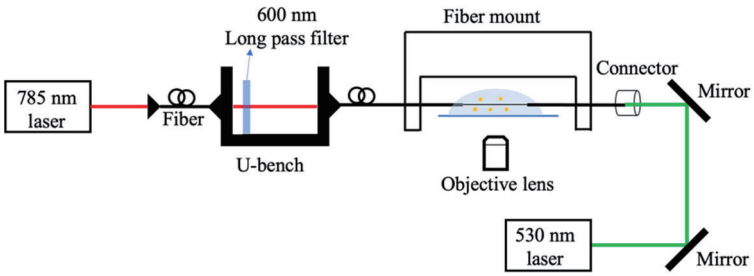

FIG. 2. The scheme of experimental setup.

Reference

[1] M. Joos, A. Bramati, and Q. Glorieux, *Opt. Express*, 27, 18818-18830 (2019).
[2] C. Lee, M. A. Buyukkaya, S. Harper, S. Aghaeimeibodi, C. J. K. Richardson, and E. Waks, *Nano Letters*, 21, 323-329 (2021).
[3] M. Sadgrove, M. Sugawara, Y. Mitsumori and K. Edamatsu, *Sci Rep*, 7, 17085 (2017).
[4] M. Sugawara, Y. Xuan, Y. Mitsumori, K. Edamatsu and M. Sadgrove, *Phys. Rev. Research*, (in press) (2022).
[5] T. Yoshino, D. Yamaura, M. Komiya, M. Sugawara, Y. Mitsumori, M. Niwano, A. Hirano-Iwata, K. Edamatsu, and M. Sadgrove, *Opt. Express*, 28, 38527-38538 (2020).

Electromagnetic-field analysis of the plasmon-enhanced single photon emitters on an optical nanofiber

Yining Xuan[1,2], Rui Sun[1,2], Soyoung Baek[1], and Keiichi Edamatsu[1]
[1]*Research Institute of Electrical Communication, Tohoku University*
[2]*Department of Electronic Engineering, Graduate School of Engineering, Tohoku University*
xuan.yining.t8@dc.tohoku.ac.jp

Single photon emitter has many applications in quantum information, communication, and metrology. Therefore, bright single photon emitters with enhanced quantum efficiency are very important for practical quantum applications and have been studied using various systems [1]. To achieve an enhanced, polarized single photon source that can be coupled into the fiber network directly, we studied on a gold nanoparticle-quantum-dot (GNP-QD) coupled system [2,4], as shown in Fig.1. The single photon source in this research is based on a semiconductor quantum dot (QD) with the emission wavelength around 800 nm. The surface plasmon resonance of gold nanoparticles (GNP) provide large Purcell enhancement relative to conventional cavities and can also provide enhancement of degree-of-polarization (DOP) depending on the type of nanoparticle. In addition, optical nanofibers have the advantages of low optical loss when coupling to conventional fiber networks, and low cost as they can be fabricated from standard single mode optical fibers. Furthermore, through the evanescent field of the nanofiber, photons from QDs can be coupled directly into the nanofiber and hence an optical fiber network.

To understand the distribution of electric field and the impact of incident light on gold nanoparticles on the nanofiber, we carried out electromagnetic-field analysis (FDTD: Finite-difference time-domain method). We analyze the background field distribution, reflection coefficient, absorption and scattering cross section of gold nanoparticles on the fiber surface at various incident angles. Through the analysis of electric field distribution and localized surface plasmon response of gold nanoparticles in Fig.2, the performance of gold nanoparticles on the surface of nanofiber is obtained and discussed. The single photon source with GNP-QD structure can enhance the luminous efficiency of quantum dot due to the Purcell effect. We plan to add a quantum dot in the vicinity of the gold nanoparticle and perform the simulation.

This work was supported by MEXT Q-LEAP Grant Number JPMXS0118067581.

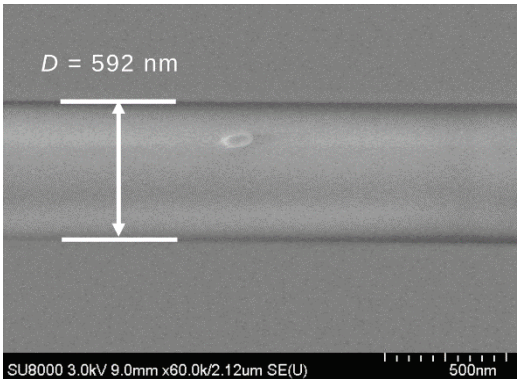

FIG. 1. SEM image of the quantum-dot-gold-nanorod coupled system on an optical nanofiber.

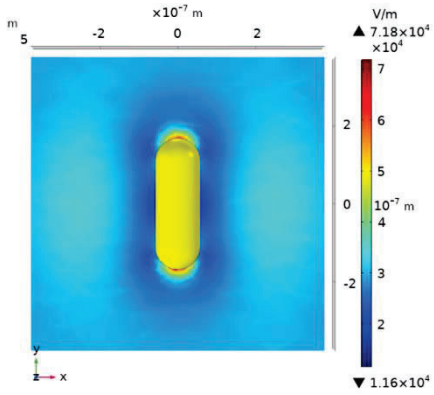

FIG. 2. Localized plasmon resonance of gold nanorod using FDTD simulation.

Reference

[1]H. J. Kimble, Nature, 453, 7198 (2008).
[2]M. Sadgrove, M. Sugawara, Y. Mitsumori, and K. Edamatsu, Sci. Rep., 7, 17085 (2017).
[3]M. Sugawara, Y. Mitsumori, K. Edamatsu, and M. Sadgrove, Opt. Express, 28, 18938 (2020).
[4]M. Sugawara, Y. Xuan, Y. Mitsumori, K. Edamatsu, M. Sadgrove, Phys. Rev. Research, (in press) (2022).

Ultrafast measurement of biphoton wave packets using optical Kerr gating

Takahisa Kuwana[1], Masahiro Yabuno[2], Fumihiro China[2], Shigehito Miki[2], Hirotaka Terai[2], Peter J. Mosley[3], Rui-Bo Jin[4] and Ryosuke Shimizu[1]

[1]*The University of Electro-Communications, 1-5-1 Chofugaoka, Chofu, Tokyo, Japan*

[2]*Advanced ICT Research Institute, National Institute of Information and Communications Technology, 588-2 Iwaoka, Nishi-ku, Kobe 651-2492, Japan*

[3]*Centre for Photonics and Photonic Materials, Department of Physics, University of Bath, Bath, BA2 7AY, UK*

[4]*Hubei Key Laboratory of Optical Information and Pattern Recognition, Wuhan Institute of Technology, Wuhan 430205, China*

k2133039@gl.cc.uec.ac.jp

Introduction

Single-photon detection is of importance for quantum information and sensing technologies. Improving the temporal resolution in single-photon detection is essential for the further development of quantum technologies. Currently, a superconducting nanowire single-photon detector has achieved ~3 ps temporal resolution, which is the best temporal resolution as far as we know. However, there is a trade-off between detection efficiency and temporal resolution. Thus, extending into the femtosecond range is challenging without a catastrophic reduction in detector efficiency. On the other hand, optical gating with ultrafast laser pulses can efficiently detect photons with high temporal resolution. Up to now, we developed an ultrafast single-photon detector using an optical Kerr gating (OKG) and demonstrated the single-photon detection with 224±9 fs temporal resolution under low-gating power consumption (~20 mW)[1]. However, no demonstration of a two-photon detection by the OKG has been reported. In this work, we present the development of our OKG system to a two-photon detection toward joint temporal intensity (JTI) measurements.

Experiment

Figure 1 shows the schematic diagram of the experimental setup. Our PCF was specially designed to minimize the group velocity difference between the photons with the center wavelength of 1584 nm and the gating pulse with the wavelength of 792 nm for efficient cross-phase modulation. Ultrafast pulses from a mode-locked Ti:sapphire laser operating at the wavelength of 792 nm were divided by a polarization beam splitter. One is sent to a periodically poled KTP (PPKTP) crystal to generate biphotons in a type-II phase-matching condition and the other is used for gating pulses of the OKG system. Biphotons generated via PPKTP crystal were led to the OKG system with the Sagnac interferometer configuration. Photons were propagated in either clockwise (CW) or counterclockwise (CCW) directions. Only the photon wave packet in the CW propagation was copropagated with the gating pulse. Then, a nonlinear phase shift by the optical Kerr effect was added to the photon overlapped with the gating pulse in the PCF. In the case that the phase difference between CW and CCW propagation of the Sagnac interferometer is not zero, a portion of the photons are outputted to the detection port. Eventually, we can measure the envelope of the wave packet by sweeping the relative delay between the photon and the gating pulses. With the help of polarization multiplexing, we developed our system to the two-photon detection. We reconstruct the JIT from coincidence counts of our Kerr gating system.

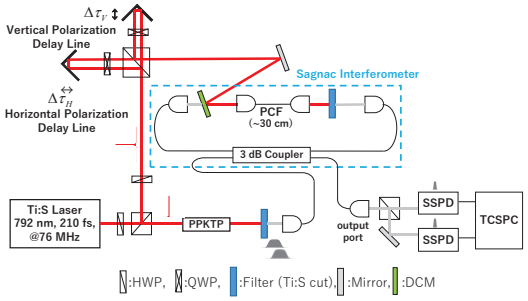

FIG. 1. JTI measured our OKG system

Results and discussion

Figure 2 shows the measured JTI. We can clearly see the two-photon temporal distribution with a negative correlation. This is the first experimental observation of the JTI by the OKG. We achieved the maximum signal-to-noise ratio with a gating power of 50 mW, meaning that the order-of-magnitude improvement of the gating power consumption compared to the up-conversion method[2].

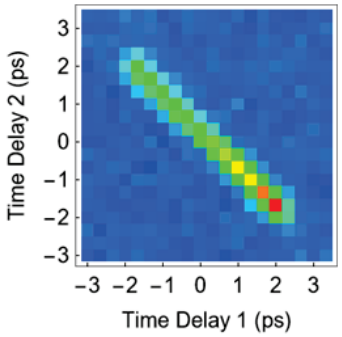

FIG. 2. JTI measured our OKG system

Acknowledgment

This work was supported by MEXT Q-LEAP Grant Number JPMXS011806924.

Reference

[1] M. Yabuno, R. Shimizu , *et al.,* Opt. Express **30**, 4999-5007 (2022).

[2] R.-B. Jin, R. Shimizu , *et al.*. Phys. Rev. Appl. **10**, 034011/1-11 (2018).

Growth of thick CVD diamond films containing aligned nitrogen-vacancy centers for high-sensitivity quantum sensors

Takeyuki Tsuji[1], Takayuki Iwasaki[1], and Mutsuko Hatano[1]

[1]*Department of Electrical and Electronics Engineering, School of Engineering, Tokyo Institute of Technology*

tsuji.t.ac@m.titech.ac.jp

A large volume of CVD diamond films containing aligned nitrogen-vacancy (NV) centers lead to highly sensitive quantum sensors. To form perfectly aligned NV centers, diamonds need to be grown using lateral growth in the [1$\bar{1}$2] direction.[1] It is necessary to cut and polish the diamond substrate at a misorientation angle (θ_{mis}) to create the steps, as shown in Fig. 1. Geometrically, as θ_{mis} increases, the maximum thickness of the diamond film increases, as shown in Fig. 1. For example, if a 1 mm^2 diamond substrate is polished at θ_{mis}=10°, the maximum film thickness is 1 mm × sin(10°) ≈ 170 µm, while at θ_{mis}=0.5°, the maximum film thickness is 1 mm × sin(0.4°) ≈ 7 µm. Therefore, θ_{mis} is a key parameter in determining the thickness of the diamond films. In this study, the dependence of the growth rate and NV center properties on θ_{mis} (= 0.4°–9.9°) was investigated for synthesizing a thick diamond film containing aligned NV centers.

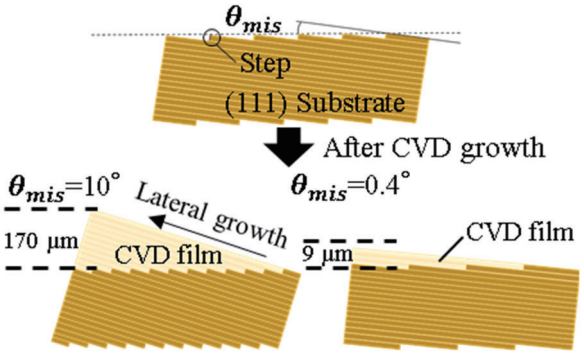

Fig.1. Differences in the maximum film thicknesses for different misorientation angles (θ_{mis}).

Diamond films containing NV centers were grown on Ib (111) diamond substrates (1 mm × 1 mm × 0.3 mm). The surfaces of the diamond (111) substrates were polished in the [1$\bar{1}$2] direction at θ_{mis} of 0.4(1) °, 2.7(1) °, 3.7(1) °, 5.0(1) °, and 9.9(1) °, which were measured using X-ray diffraction. We used a high-power density MPCVD where the microwave plasma was reflectively concentrated above the diamond substrates by a spherical chamber.[2] Hydrogen, methane, and nitrogen gases flowed in the setup at 500, 0.5, and 0.01 sccm, respectively. The pressure, microwave power, and temperature were set to 30 kPa, 2.1 kW, and 800 °C, respectively. The thickness and nitrogen density of the diamond films were measured using secondary ion mass spectrometry (SIMS). The fluorescence of the NV centers was measured using a home-built confocal microscope.

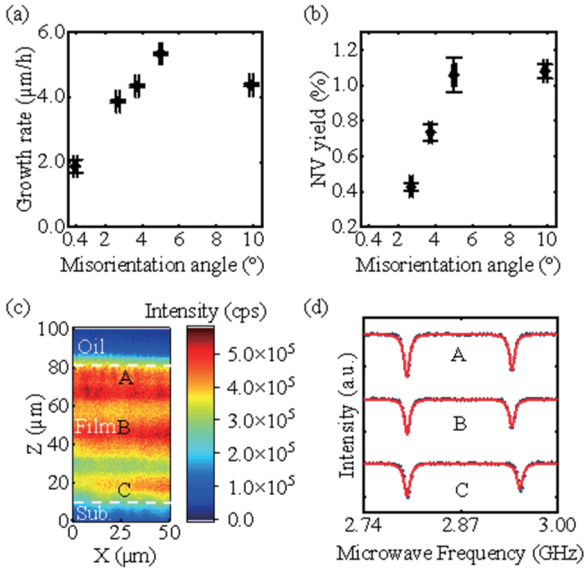

Fig.2. (a)–(b) Dependence of the growth rate and NV yield on misorientation angles, respectively. (c) Cross-sectional image of the CVD diamond film using the confocal microscope. (d) CW-ODMR spectra of the CVD diamond film at different positions shown in (c).

The growth rate increased from 1.8 µm/h to 5.3 µm/h when θ_{mis} increased from 0.4° to 5.0°, and it was 4.4 µm/h at 9.9°.(Fig.2. (a)) This was discussed by the relationship between a migration length of carbon precursors and a terrace width. With increased θ_{mis}, the NV yield, a fraction of the NV center density in the nitrogen density, increased from 0.4% to 1.1%. (Fig.2. (b)) Finally, a diamond film was synthesized for 30 h to obtain a thick diamond film using the 1 mm^2 diamond substrate with θ_{mis}=9.9°. Figure 2(c) shows a cross-sectional image of the CVD diamond film. Considering the refractive index of diamond (2.41) and immersion oil (1.52) and the numerical aperture (NA) of the objective lens (1.42), the distance of the detection point moved in the CVD diamond film was 1.71 times the distance the objective lens moved.[3] Thus, the film thickness was calculated as approximately 70 µm (CVD film thickness seen by an X-Zscan) × 1.72 ≈ 120 µm. Figure 2(d) shows the CW-ODMR spectra of the film at different positions shown in Fig. 5(g). Only two CW-ODMR peaks were observed, which confirmed the formation of perfectly aligned NV centers throughout the thick diamond film. This study is useful to design high-sensitivity diamond films using NV centers.

Acknowledgment This work was supported by MEXT Q-LEAP Grant Number JPMXS0118067395. and conducted at (NanofabPF, Tokyo Tech), supported by "Nanotechnology Platform Program" of the Ministry of Education, Culture, Sports, Science and Technology (MEXT), Japan, Grant Number JPMXP09F-21-IT-014.

Reference [1] T. Miyazaki, et al., Appl. Phys. Lett. 105, 261601 (2014).[2] T. Tsuji, H. Ishiwata, T. Sekiguchi, T. Iwasaki and M. Hatano, Diam. Relat. Mater. [108840], 108840 (2022). [3] E. E. Diel, J. W. Lichtman and D. S. Richardson, Nat. Protoc. 15 [9], 2773 (2020).

Enhancement of fluorescence collection efficiency using angle-shaped diamonds for compact magnetic sensor

Yuta Shigenobu[1], Yuta Kainuma[1], Yuji Hatano[1], Takayuki Shibata[2]
Akimichi Nakazono[3], Takeshi Ohshima[4], Mutsuko Hatano[1,4], Takayuki Iwasaki[1]
[1]*Department of Electrical and Electronics Engineering, Tokyo Institute of Technology*
[2]*DENSO CORPORATION,*
[3]*YAZAKI CORPORATION,*
[4]*National Institutes for Quantum Science and Technology*
shigenobu.y.aa@m.titech.ac.jp

Introduction

Nitrogen-vacancy (NV) centers in diamond work as highly sensitive magnetic field sensors with a wide dynamic range, a wide operating temperature range, and the ability to simultaneously measure magnetic field and temperature, which are suitable for applications of battery monitoring[1] and biomedical sensing[2]. In order to improve the magnetic field sensitivity, it is important to develop a method to collect red fluorescence emitted from NV centers in a diamond sensor with high efficiency. A Compound Parabolic Concentrator (CPC) lens[3] has been utilized to increase the collection efficiency. In this study, we propose a new method, which can be combined with the CPC lens, for the enhancement of the collection efficiency using a three-sided-angle-shaped diamond. We found that the efficiency can be more than doubled with a side angle of 30° or higher.

Method

The sensor head used in the experiment and simulation model is shown in Fig.1, where the distance (t) between the CPC lens and the Photo Detector (PD) light-receiving surface is variable from 1.75 mm to 11.75 mm. First, we used light path analysis software (LightTools) to simulate the fluorescence collection efficiency (β_{sim}) when the diamond side shaping angle θ was increased from 0° to 50° with a step size of 10°. Experimentally, a green laser (wavelength: 532 nm) was irradiated to be perpendicular to the (111) plane of the diamond sensor, and PD current was measured. The diamond sensors used were HPHT-grown Ib (111) substrates ($2.0\times2.0\times0.6$ mm^3). The NV centers were formed by irradiating with an electron beam with a fluence of 1.0×10^{18} cm^{-2} and subsequently annealing at 1000 °C for 2 hours. Then, the sidewalls of the samples were angle-polished.

Result

Figure 2(a) shows the simulated β_{sim} while changing the side-angle and distance between the CPC lens and light-receiving surface of PD. β_{sim} decreases as increasing the distance. Thus, we investigated the dependence of β_{sim} on the grinding angle at a short distance of 1.75 mm. The inset of Fig. 2(a) shows that β_{sim} increased in the range from 0° to 20°, while it remained approximately constant from 20° to 40°. The comparison between 0° and 30° polishing shows the increase in β_{sim} by a factor of about 2. The further increase in the angle above 40° again makes β_{sim} higher. Then, we performed the experiments using two samples of 0° and 30° shaping. Figure2(b) depicts the measured PD current as a function of the green laser power. The PD current of the 30° polished sample becomes 2.4 times higher compared to the 0° sample, which agrees with the simulation.

This work was supported by MEXT Q-LEAP Grant Number JPMXS0118067395.

References

[1] Y. Hatano et al., Sci. Rep. 12, 13991 (2022) [2] K. Arai et al, Commun Phys 5, 200 (2022)
[3] T. Wolf et al., Phys. Rev. X **5**, 041001 (2015).

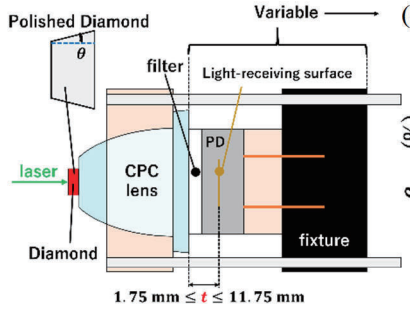

Fig.1 Sensor head structure

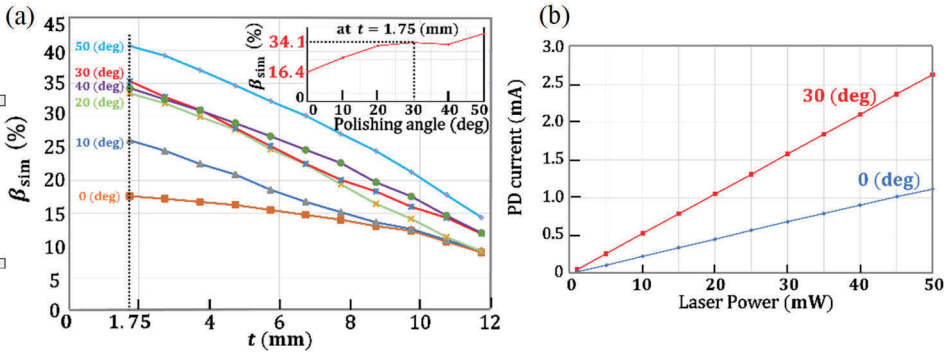

Fig.2 (a) Simulation of $\beta_{sim.}$ depending on the polishing angle and PD position. (b) Experimentally obtained PD current for the 0° and 30° samples.

Transfer-printing-based integration of SiN grating structure on diamond toward highly sensitive quantum sensor

Ryota Katsumi[1, 2], Takeshi Hizawa[1], Akihiro Kuwahata[2, 3], Shun Naruse[1], Yuji Hatano[4], Takayuki Iwasaki[4], Mutsuko Hatano[4], Fedor Jelezko[5], Shinobu Onoda[6], Takeshi Ohshima[6], Masaki Sekino[2], and Takashi Yatsui[1, 2]

[1] *Graduate School of Engineering, Toyohashi University of Technology*
[2] *Graduate School of Engineering, The University of Tokyo*
[3] *Graduate School of Engineering, Tohoku University*
[4] *School of Engineering, Tokyo Institute of Technology*
[5] *Institute of Quantum Optics, Ulm University*
[6] *National Institutes for Quantum Science and Technology*

katsumi.ryota.ti@tut.jp

Introduction

A nitrogen-vacancy (NV) center in diamond is one of the promising candidates for quantum sensing, especially sensitive magnetic sensing thanks to their excellent spin property[1,2]. However, their demonstrated magnetic field sensitivity is far beyond that based on conventional magnetometers including superconducting quantum-interference devices. One of the critical issues is the poor extraction efficiency of the emitted photons from the diamond NV substrate[3]. This can be overcome by implementing the nanostructure on diamond including gratings, but the fabrication of such structure on diamond has the technical difficulty.

Method and Result

In this work, we demonstrate the hybrid integration of a silicon nitride (SiN) circular grating structure on a single-crystal diamond NV substrate toward sensitive magnetometers. Figure 1(a) displays an SEM image of the grating based on SiN, which is transparent for the NV emission wavelength of ~700 nm. To pick them up, we employed the air-bridged structure for the grating. By using the pick-and-place transfer printing[4] [Fig. 1(b)], the SiN grating was integrated on the diamond NV substrate. Figure 1(c) displays an optical microscope image of the fabricated device. The SiN grating is bonded with the diamond NV substrate.

The fabricated device was characterized using micro-photoluminescence (μPL) spectroscopy. The NV centers were excited with a 532 nm-CW laser. The red curve in Fig. 1(d) shows a PL spectrum measured for the sample with the SiN grating at an input laser power of 12 mW. For comparison, we measured the PL spectrum for the bare region of the diamond NV substrate near the SiN grating (blue curve in Fig. 1(d)). The collected photon counts are increased by a factor of up to 1.6 with the SiN grating structure. We also evaluated the magnetic sensitivity of the fabricated device. Figure 1(e) shows the lock-in voltage detected by the lock-in detection system[2] as a function of the magnetic field strength *B*. The detected voltages with the grating are higher than those in the bare region, which is consistent with the results of Fig. 1(d) and demonstrating the improvement of the magnetic sensitivity in the fabricated device.

Acknowledgement

This work was supported by MEXT Q-LEAP Grant Number JPMXS0118067395 and Kakenhi (20H02197, 20H05091, 20K21118, 21K20428, 22H01525, and 22K14289).

References

[1]J. M. Taylor, *et al.,* Nat. Phys. **4**, 810 (2008).
[2]A. Kuwahata, *et al.,* Sci Rep **10**, 2483 (2020).
[3]D. Le Sage, *et al.,* Physical Review B **85**, 121202 (2012).
[4]R. Katsumi, *et al.,* Optica **5**, 691 (2018).

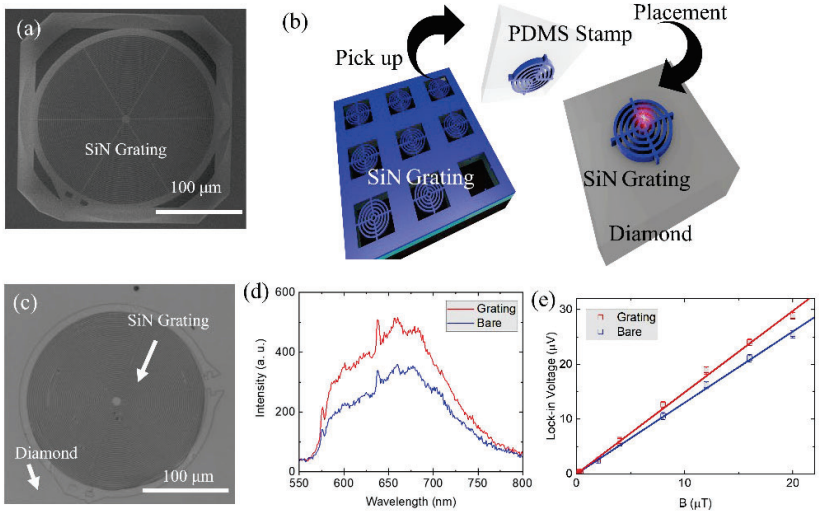

FIG. 1. (a) SEM image of the fabricated SiN grating. (b) Schematics of transfer printing of SiN grating on diamond. (c) Optical microscope image of the fabricated device. (d) Measured PL spectra (red: SiN grating, blue: bare region). (e) Lock-in voltage detected by the lock-in detection system as a function of magnetic field strength (B).

NVC-SPM System to Inspect Electric Devices

Teruo Kohashi[1], Masanari Koguchi[1], Akehito Shiotake[2] and Satoshi Ono[2]

[1]*Hitachi, Ltd., Research & Development Group, Hatoyama, Saitama, 350-0395 Japan*

[2] *The Graduate School of Informatics and Engineering, The University of Electro-Communications, Choufu, Tokyo, 182-8585, Japan*

teruo.kohashi.fc@hitachi.com

Introduction

A scanning probe microscope using nitrogen-vacancy color centers in diamond (NVC) as a probe (NVC-SPM) has been developed [1,2], taking advantage of excellent characteristics of NVC, such as high sensitivity for magnetic field detection in three dimensions and high spatial resolutions. For now, this technique is mainly used to study fundamental physical phenomena. On the other hand, we are developing an NVC-SPM to inspect electric devices by evaluating magnetic fields generated from a tiny electric wiring. In this paper, we report the development of a new system including a compact microwave antenna and mini-mirror, which makes it possible to inspect the predetermined electric circuit in a wide circuit board.

Results

It is important to set the microwave antenna as close as fifty μm to the probe in NVC-SPM, referring to the previously published example [2]. In order to detect magnetic field generated around a minute wiring between the pads, the microwave antenna should be inserted between the two electrical pads, which are positioned in the distance of less than 1mm. Moreover, irradiation and detection light are performed with a confocal microscope with a working distance of 4.5 mm. It means that the antenna and the probe should be set above the predetermined electric circuit in the space of 4.5mm. We need to set these components precisely in the measurement; therefore, it is desired to confirm the position of each component in the vertical direction from the sample surface. However, the field of view is very narrow through the objective lens (e.g., several hundred μm) because the lens center diameter is very small. A new function for precise position adjustment among these components was required in our SPM system.

Our new NVC-SPM is summarized in Fig. 1. We designed the microwave antenna with very tiny coil with diameter of 500μm, and mini-mirror to confirm the position of each component from vertical direction using a camera. We developed the above-mentioned system as shown in Fig. 2, and confirmed that this system works properly. As a next challenge, we will inspect the actual electric circuit using this NVC-SPM system.

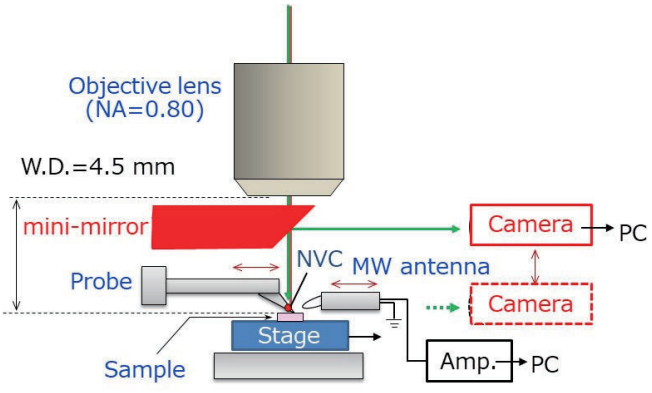

FIG. 1. Newly developed NVC-SPM system with mini-mirror.

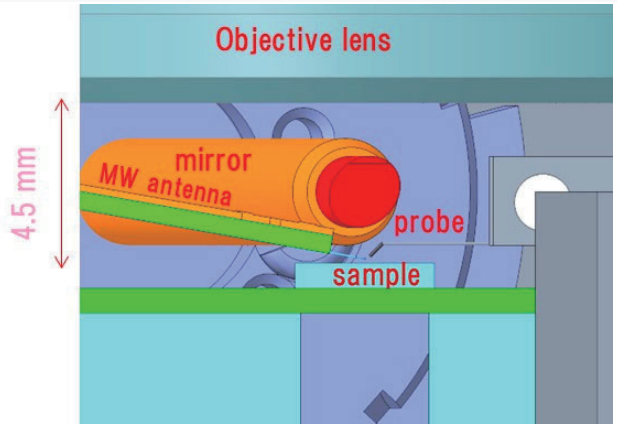

FIG. 2 3D-CAD image of set up around the sample.

This work was supported by MEXT Q-LEAP Grant Number JPMXS0118067395.

Reference

[1] J. M. Taylor, P. Cappellaro, L. Childress, L. Jiang, D. Budker, P. R. Hemmer, A. Yacoby, R. Walsworth, M. D. Lukin, Nat. Phys. **4**, 810 (2008).

[2] T. X. Zhou, R. J. Stohr and A. Yacoby, Appl. Phys. Lett 111, 163106(2017).

Enhancing sensitivity with entanglement in coupled nitrogen vacancy centres

Ernst David Herbschleb[1], Riku Kawase[1], Hiroyuki Kawashima[1], Hiromitsu Kato[2], Toshiharu Makino[2], Satoshi Yamasaki[3], Shinobu Onoda[4], Hiroshi Abe[4], Takeshi Ohshima[4], Norikazu Mizuochi[1]

[1]*Institute for Chemical Research, Kyoto University*
[2]*National Institute of Advanced Industrial Science and Technology (AIST)*
[3]*Nanomaterials Research Institute, Kanazawa University*
[4]*National Institutes for Quantum Science and Technology (QST)*
herbschleb@dia.kuicr.kyoto-u.ac.jp

Introduction

Quantum sensing has great potential for applications that require ultra-high sensitivities. The nitrogen-vacancy (NV) centre is an important example of a quantum sensor, since it works under ambient conditions, enables high spatial resolution, and several physical quantities can be measured. Coherence is a quantum resource that is already utilised in many quantum sensing protocols. However, the ultimate quantum resource, entanglement, has yet to see use. This could enhance the sensitivity significantly, but it is far from straightforward.

Method

In our research, to create NV centres that have a high chance to be coupled, we implant molecules with multiple nitrogen atoms into diamond samples, such that the distance between potential NV centres is dictated by straggling only [1]. By choosing phosphorus-doped diamond ([P] ≈ 5 x 10^{15} cm^{-3}, created via CVD with enriched ^{12}C [2]), we expect to have a higher yield [3], and hence a higher chance to find NV centres with a strong coupling. Moreover, the coherence time is potentially longer [3], which is important for various quantum protocols.

We compare results between intrinsic diamond and phosphorus-doped diamond, for which initial results show an increase in yield (Fig. 1). Moreover, the number of spots with more than one NV centre is consistent with the yield per nitrogen atom; an example ODMR spectrum is shown in Fig. 1. Double electron-election resonance experiments give the coupling strength between NV centres, which needs to be sufficiently strong to attempt to utilise a couple for enhanced sensing.

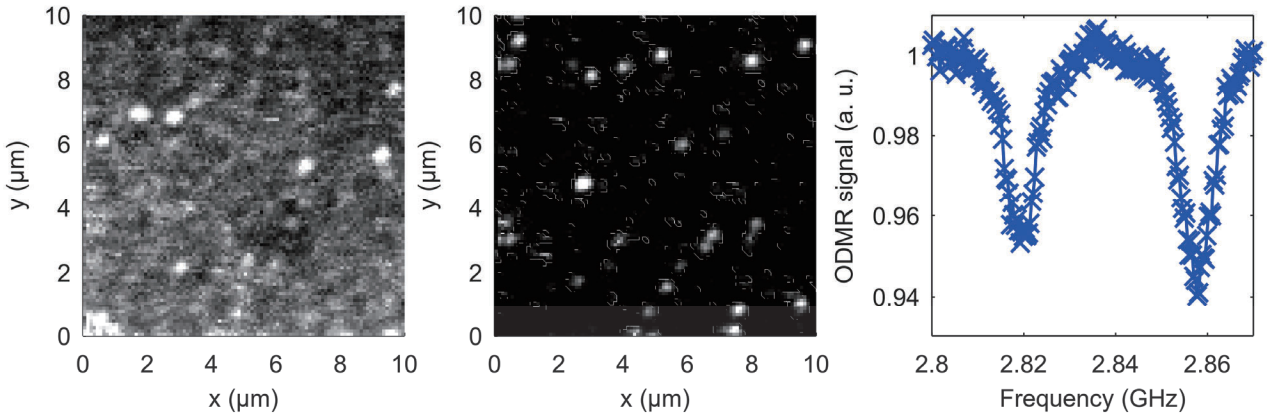

FIG. 1. (Left) Confocal microscope image for intrinsic diamond, showing less than 10 spots with NV centres. (Middle) Confocal microscope image for phosphorus-doped diamond implanted with the same parameters as intrinsic diamond. There are over 20 spots with NV centres. Moreover, the photon count per NV centre is higher compared to the intrinsic sample. (Right) Optically detected magnetic resonance (ODMR) image for a spot with two NV centres with a different orientation.

Acknowledgement

This work was supported by MEXT Q-LEAP Grant Number JPMXS0118067395.

References

[1]Haruyama et al., Nature Communications 10, 2664 (2019).
[2]E. D. Herbschleb et al., Nature Communications 10, 3766 (2019).
[3]A. Watanabe et al., Carbon 178, 294-300 (2021).

Frequency-bin generation of entangled photons via quantum optical synthesis

Takeru Naito[1], Masahiro Yabuno[2], Fumihiro China[2], Shigehito Miki[2], Hirotaka Terai[2], and Ryosuke Shimizu[1]

[1] *The University of Electro-Communications, 1-5-1 Chofugaoka, Chofu, Tokyo, Japan*

[2] *Advanced ICT Research Institute, National Institute of Information and Communication Technology, 588-2 Iwaoka, Nishi-ku, Kobe Japan*

n2133076@uec.ac.jp

Introduction

Entangled photons in high-dimensional Hilbert space are expected to increase information capacity. Although there are several approaches to realize such a high-dimensional state of the entangled photons, frequency-bin encoding is suitable for optical-fiber-based communication systems with wavelength multiplexing technologies. Up to now, frequency-bin state generation has been reported in some physical systems; Micro-ring resonators [1] and domain structure engineering of quasi-phase-matched devices [2]. However, most of the physical characteristics of the frequency-bin state are determined by the designed device structures. Therefore, it may be difficult to precisely adjust the frequency-bin state to the communication system. On the other hand, we reported manipulating the time-domain structure of a biphoton wave packet via Fourier optical synthesis in the frequency domain and realized an ultrafast time-bin state of the biphoton wave packet in several pico-second ranges [3]. Since the Fourier optical approach is independent of the device structure, it would provide better flexibility in manipulating the time-frequency structure of the biphoton wave packet. In this study, we present a proof-of-concept experiment of a two-photon spectral modulation with Fourier optical synthesis (FOS) toward the frequency-bin state generation with high flexibility.

Experimental results

In this experiment, photon pairs are generated by spontaneous parametric down-conversion using a periodically poled MgO-doped stoichiometric $LiTaO_3$ (PPMgSLT) crystal. In the earlier experiment with the PPMgSLT, broadband joint spectral intensity (JSI) distribution with negative correlation was reported even under a type-II phase-matching condition. Based on this scheme, we develop a spectral manipulation technique by Fourier optical synthesis in the time domain. Since discrete joint temporal intensity (JTI) distributions are needed for our synthesis, we adopt a bidirectional pumping scheme to the PPMgSLT crystal by reflecting the pump pulse by a concave mirror. As a result, a sequential JTI distribution with positive temporal correlation is created. For further manipulation, we placed a dichroic mirror between the PPMgSLT and the concave mirror to separate the biphoton wave packet, created by the first pumping, from the pump pulse. Adjusting a mirror position for the biphoton wave packet, we can control the temporal separation of the two biphoton wave packets along anti-diagonal direction. Photon pairs from the bidirectional pumped source were collected into a polarization-maintaining fiber and were sent to a fiber-based spectrometer. We reconstructed JSIs from the arrival time of photons after passing through the spectrometer. Photons were detected by superconducting single-photon detectors.

Figure 1 represents the resultant JSI when the two JTIs are distributed parallel to each other to the diagonal direction defined by $\Delta\tau_s = -\Delta t_i$. We can see the JSI is modulated along the anti-diagonal direction defined by $\Delta\nu_s = -\Delta\nu_i$ and it forms a frequency-bin state. The product of these modulation periods of each bin and interval of the two JTI is $\Delta t_- \cdot \Delta\nu_- \cong 1.3$, meaning successful demonstration of the FOS in the time domain.

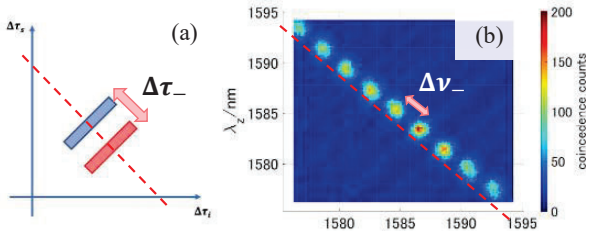

FIG.1. (a)Expected JTI (b) Measured JSI formed the frequency-bin state.

Acknowledgement

This work was supported by MEXT Q-LEAP Grant Number JPMXS011806924.

Reference

[1] C. Joshi, A. Farsi, A. Dutt, B.Y.Kim, X. Ji, Y. Zhao, A.M. Bishop, M. Lipson, and A.L. Gaeta, "Frequency-Domain Quantum Interference with Correlated Photons from an Integrated Microresonator," Phys. Rev. Lett. **124**, 143601/1-7 (2020).

[2] C.L. Morrison, F. Graffitti, P. Barrow, A. Pickston, J. Ho,and A. Fedrizzi, "Frequency-bin entanglement from domain-engineered down-conversion" APL Photonics **7**, 066102 (2022).

[3] R.B. Jin, K. Tazawa, N. Asamura, M. Yabuno, S. Miki, F. China, H. Terai, K. Minoshima, and R. Shimizu, "Quantum optical synthesis in 2D time-frequency space," APL Photonics **6**, 086104/1-7 (2021).

Development of highly sensitive gravimeter based on atom interferometry using hybrid system for field applications

Takeshi Hojo, Kaito Takamura, and Ken'ichi Nakagawa
Institute for Laser Science
University of Electro-Communication
t_houjo@ils.uec.ac.jp

Introduction

Transportable gravimeters with the sensitivity of about few micro Gal (10^{-9} g) are required in the fields of geophysics and geodesy. As the atom gravimeters have favorable features for these fields such as high sensitivity and no moving elements, they will contribute to these fields. We have developed a transportable gravimeter for these fields. Our experimental setup is shown in Fig.1. In our experiment, using retro-reflected three-beam MOT, about 10^7 laser cooled ^{87}Rb atoms are loaded in a glass cell. One of problems to limit the sensitivity of the atom gravimeters is the vibrational noise from the floor through the retro-reflecting mirror of Raman beams (Fig. 1). Therefore, the low frequency (< 10 Hz) vibrational noise of the mirror should be suppressed by using passive or active vibrational systems to achieve the target sensitivity of the gravity measurement. In our gravimeter system, we use a commercial passive isolation system with a resonance frequency of about 0.5 Hz, and we can improve the signal to noise ratio of the interference fringe (Fig, 2). Without a vibrational isolator, we could not clearly observe the interference signal for the interaction time longer than 30 ms. By employing a vibrational isolator, we could observe the interference signal for the interaction time up to 45 ms, and the sensitivity of $\Delta g/g = 7.2 \times 10^{-8}$ was realized. However, a residual vibrational noise limits the sensitivity and we could not further improve the sensitivity. To improve the sensitivity further, we consider a hybrid approach in which both the atom gravimeter and the mechanical accelerometer are employed to improve the sensitivity [1]. To realize this hybrid system, we first examined the correlation between the signals from the atom gravimeter and the mechanical accelerometer. The phase shift of the observed interference signal and the shift estimated from the accelerometer are plotted in Fig. 3, and we could observe the correlation between both signals. Using the high correlation between both signals, the phase of the interference signal is compensated by the phase shift estimated from the mechanical accelerometer signal, and we will be able to further improve the sensitivity of the gravity measurement.

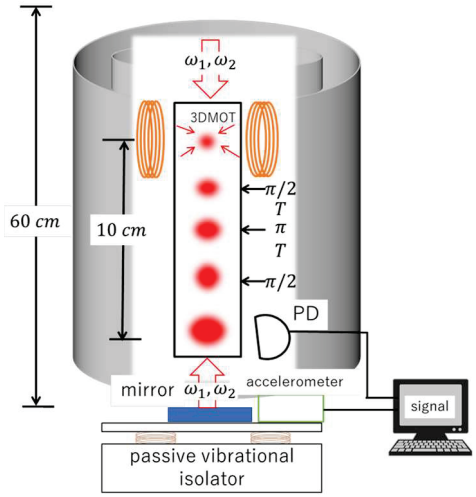

FIG 1. Experimental setup.

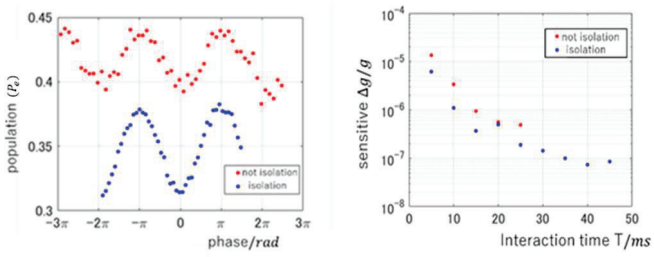

FIG 2. Interference signals without(red) and with vibrational isolation(blue)

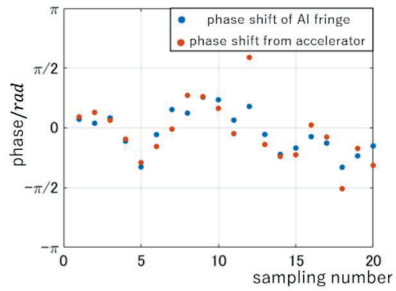

FIG3. Phase shifts of the interference signal (blue) and the accelerometer (orange)

Acknowledgement

This work was supported by MEXT Q-LEAP Grant Number JPMXS0118069452

Reference

[1] Aopeng Xu, "vibration compensation of an atom gravimeter", Chinese Optics Letters Vol. 17, Issue 7, 070201(2019)

Implementation of Double Quantum Magnetometry to Continuously Excited Ramsey Method

Yuta Araki[1], Ikuya Fujisaki[1], Yuji Hatano[1], Takeharu Sekiguchi[1], Takayuki Shibata[2], Takayuki Iwasaki and Mutsuko Hatano[1]

[1]*Department of Electrical and Electronics Engineering, School of Engineering, Tokyo Institute of Technology*

[2]*DENSO Corporation*

araki.y.aj@m.titech.ac.jp

Introduction

NV centers, spin qubits in diamond, have been studied for magnetic sensing applications. The continuously excited (CE)-Ramsey method reported high sensitivity of $17\mathrm{pT}/\sqrt{\mathrm{Hz}}$ for DC magnetometry[1]. However, for the measurement of magneto-encephalo-graphy (MEG) in humans, which is our measurement target, further improvement in sensitivity is needed. The double quantum magnetometry (DQ) is a method to improve the DC field sensitivity[2]. Applying DQ to the conventional Ramsey measurement not only effectively doubles the NV gyromagnetic ratio, but also improves T_2^* due to common-mode noise rejection. We report the development of a measurement protocol in which DQ is applied to the CE-Ramsey method to improve the sensitivity of the DC magnetic field.

Method

The diamond sample was 110-μm-thick ^{12}C CVD layer deposited on a type IIa substrate, and was irradiated with electron beams of 5×10^{17} cm^{-2} and annealed. P1 and NV center concentrations were estimated to be approximately 8 ppm and 0.8 ppm. The static magnetic field of 10 mT was aligned parallel to the NV axis. A 532 nm laser was irradiated from the side of the sample. The fluorescence was focused by a CPC lens and read by a photodetector. To implement DQ, we applied the MW frequencies resonant to the low-frequency $m_s = 0 \leftrightarrow -1$ transition and the high-frequency $\mathrm{m_s} = 0 \leftrightarrow +1$ transition simultaneously. The single-quantum (SQ) Rabi frequencies for the two transitions were matched.

Result

CE-SQ-2-Ramsey and CE-DQ-4-Ramsey were performed to confirm the effect of DQ in the CE protocol. Compared to SQ, twice the frequency of oscillation was obtained in DQ [see Fig.1 (a)], confirming that a doubling of the NV gyromagnetic ratio was achieved. Dephasing time T_2^*, fitted values, were similar for SQ and DQ, confirming that common-mode noise rejection was achieved [see Fig.1 (a)]. Next, to confirm the effect of DQ on sensitivity enhancement, we compared the measurements of sweeping of detuning, which corresponds to an external magnetic field, between SQ and DQ. The results confirmed that the slope was improved by the application of DQ [see Fig.1 (b)].

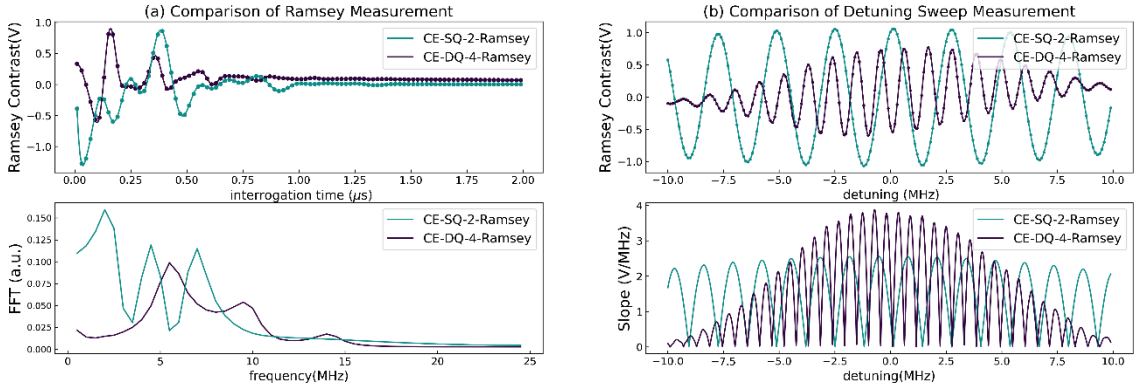

FIG. 1. (a) Comparisons of NV Ramsey measurements (Upper) and Discrete Fourier transform (Lower). (b)Comparisons of Detuning sweep measurements of SQ and DQ (Upper) and their calculated Slopes (Lower).

Acknowledgements

This work was supported by MEXT Q-LEAP Grant Number JPMXS0118067395.

We thank Dr. Hiromitsu Kato (AIST) and Dr. Shinobu Onoda, Dr. Takeshi Ohshima (QST) for supplying diamond samples.

Reference

[1]C. Zhang, *et al, Phys Rev Appl,* **15**, 1 (2021)

[2]E. Bauch *et al., Phys Rev X* , **8**, 31025 (2018)

Development of highly sensitive compact quantum sensor with NV center in ^{12}C-enriched CVD diamond for bio-medical and industrial application

Yuta Kainuma[1], Yuta Shigenobu[1], Yuji Hatano[1], Takayuki Shibata[2], Akimitchi Nakazono[3], Hiromitsu Kato[4], Takeshi Ohshima[5], Takayuki Iwasaki[1], and Mutsuko Hatano[1,5]

[1]*Department of Electrical and Electronics Engineering, School of Engineering, Tokyo Institute of Technology*
[2]*DENSO CORPORATION*
[3]*YAZAKI CORPORATION*
[4]*National Institute of Advanced Industrial Science and technology*
[5]*National Institutes for Quantum Science and Technology*
kainuma.y.aa@m.titech.ac.jp

Introduction

Magnetometers based on the ensemble nitrogen-vacancy (NV) centers have high magnetic sensitivity and have monitored not only rat's cardiac magnetism[1] but also battery current over a wide dynamic range[2]. For these applications, especially, magnetoencephalography have required high magnetic sensitivity and multiple sensors. Thus, the development of a compact quantum sensor is important to be implemented in the system with sufficient spatial resolution. However, these sensors have not achieved the magnetic sensitivity required to detect magnetoencephalography.

We investigated the magnetic sensitivity of the quantum sensor head by lateral laser irradiation using ^{12}C-enriched chemical vapor deposition (CVD) growth diamond, which is suitable for NV centers and scalable device fabrication.

Method

Figure 1(a) shows the construction of the quantum sensor head, the inside of the dashed line is an NV diamond; The NV centers in ^{12}C-enriched CVD diamond were formed by electron-beam irradiation (5.0×10^{17} e/cm^2) and high-temperature annealing after it. The excitation green laser (wavelength: 532 nm) was focused on the side of the NV diamond by a lens (focal length: 200mm). The photoluminescence from the NV center collected by compound parabolic concentrator (CPC) lens and split laser by the beamsplitter in the optical line are detected by a photodiode (PD1) and PD2 as shown in Fig.1(a). A laser-noise compensation is performed by an auto-balance (AB) circuit and the output signal is modulated by a lock-in amplifier (LIA) with the modulation frequency (f_{mod}) = 7.03 kHz. The magnetic field was adjusted to be parallel to the NV quantum axis. The resonance frequency of the lock-in optically detected magnetic resonance (ODMR) spectra was locked by the output microwave frequency updated. The optical setup was assembled in the magnetic shield.

Result and discussion

The measured signal spectra are shown in Fig.1(b). the floor noise of on- and off-resonance was estimated less than 60 pT/Hz$^{0.5}$ and 40 pT/Hz$^{0.5}$, however, electronic noise matched the off-resonance noise at 1 Hz. We confirmed that floor-noise attenuation in the on-resonance spectra at low frequencies seems that the feedback circuit captures the resonance frequency of ODMR. From the long-measured magnetic signal, the minimum detectable magnetic field (MDMF) was extracted with Allan variance, reaching approximately 260 fT. MDMF can be improved by faster feedback circuit and NV diamond quality; the use of preferentially-aligned NV center CVD diamond improves the magnetic field sensitivity by a factor of about 3 or more[3].

Acknowledgments This work was supported in part by MEXT Q-LEAP Grant Number JPMXS0118067395.

References [1] K. Arai et al., Commun. Phys. **5**, 200 (2022), [2] Y. Hatano et al., Sci. Rep. **12**, 13991 (2022), [3] C. Osterkamp et al., Sci. Rep. **9**, 5786 (2019)

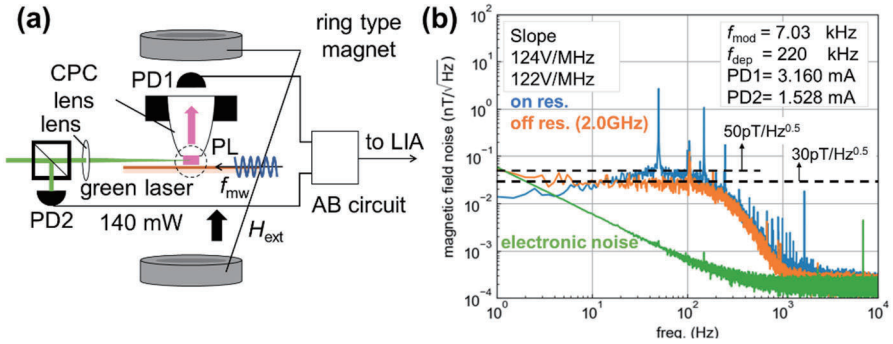

Fig .1 (a)A schematic of the construction of quantum sensor head: dashed line indicates NV diamond sensor. The diamond was glued to the apex of the CPC lens by optical adhesives. (b) Measured FFT spectrum of magnetic sensitivity. The off-resonance was measured with a microwave (f_{mw} = 2.0 GHz) applied. Electronic noise was measured without a laser.

Development of a Nonmagnetic Helical Sensor Drive Multipoint Measuring Mechanism for Magnetocardiography in Animals

Wenyu Shang[1], Motofumi Fushimi[1], Shinichi Chikaki[1], Masaki Sekino[1]
[1]*Graduate School of Engineering, The University of Tokyo*
Shangwenyu720@g.ecc.u-tokyo.ac.jp

Introduction

In the clinic, electrocardiography (ECG) and magnetocardiography (MCG) are widely known as common techniques to observe the electrophysiological activity of the heart. Because the magnetic permeability is more uniform than the conductivity in the organism, to obtain more accurate cardiac electrical information, MCG usually shows higher accuracy and specificity than ECG. (for some diseases) [1]. This study will focus on MCG technology. By introducing a new type of helical nonmagnetic measurement device, taking animals as the measurement target, we can obtain all-around magnetic field information to complete the depth measurement of the cardiac current source and realize 3D reconstruction.[2]

Methods

In this study, we proposed a new sensor array for MCG measurement in animal to obtain more depth information about current sources. Unlike conventional devices, we used a ring-shaped sensor array instead of a flat plane sensor array. We designed a mechanism to realize multipoint MCG measurement and assembled it with nonmagnetic material, as shown in Figure 1. With this mechanism, MCG data were measured using 3 OPMs.

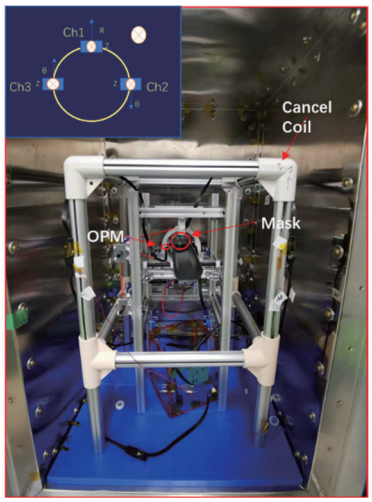

Figure 1. Multipoint MCG measurement mechanism

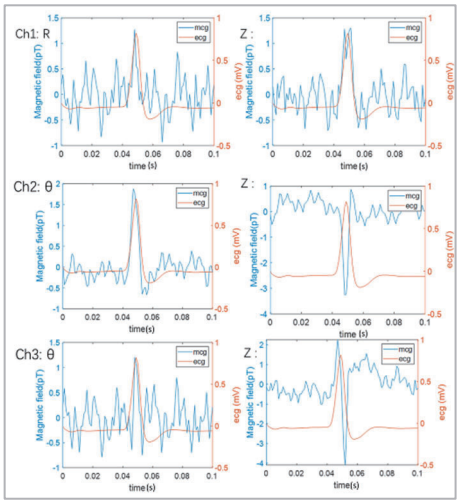

Figure 2. Result of MCG measurement in rat

Results and discussion

Figure 2 shows the results of MCG measurement. 3 OPMs with six channels were used to measure the rat's MCG. The two channels of OPM respectively detected the r and θ direction of ring. The result of additive averaging based on the simultaneously acquired ECGs shows that the R wave can be clearly captured from directions other than the anterior chest plane. However, its signal strength is weak (about 2 pT), and the design of the mechanism needs to be improved to obtain a signal with a higher signal-to-noise ratio.

Acknowledgments

This work was supported by MEXT Q-LEAP Grant Number JPMXS0118067395.

Reference

[1] Shin, et al. (2019). Clinical Hemorheology and Microcirculation, 73(2), 283-291.
[2] R. Fenici, *Expert Rev. Mol. Diagn.*, vol. 5, no. 3, pp. 291–313, May 2005.

Ensemble NV- center in diamond for quantum sensing created by high fluence electron beam irradiation

Shuya Ishii[1,2], Seiichi Saiki[1], Shinobu Onoda[1,2], Yuta Masuyama[1], Hiroshi Abe[1,2], Takeshi Ohshima[1,2]

[1]*Takasaki Advanced Radiation Research Institute, National Institutes for Quantum Science and Technology, 1233 Watanuki, Takasaki, Gunma 370-1292, Japan*, [2]*Institute for Quantum Life Science, National Institutes for Quantum Science and Technology, 4-9-1 Ana-gawa, Inage-ku, Chiba 263-8555, Japan*
ISHII.shuya@qst.go.jp

Introduction

NV^- center has been paid attention as a quantum sensor for highly sensitive detection of magnetic field, electric field, temperature and strain, etc. [1]. Electron beam irradiation followed by subsequent thermal annealing is known as the effective procedures to create NV^- center in diamond. The electron irradiation generates vacancies in diamond and the annealing enables vacancies to diffuse in the lattice. Then diffused vacancies are captured by nitrogen atoms, and as a result, NV centers are created. In addition, substitutional nitrogen atom at a lattice site (P1 center) also acts as a donor for NV center, the charge state of NV centers changes from neutral (NV^0) to NV^-. Creation high concentration of ensemble NV- centers is needed to achieve high sensitively sensing [1]. The magnetic sensitivity is proportional to the reciprocal of the number of NV centers and T_2 (spin coherence time), i.e., high concentration NV^- centers with long T_2 increase the sensitivity. P1 center has an important role for being a component of NV^- centers and acting as donor to the NV center. But it also plays a role as decoherence source (decrease in magnetic field sensitivity) [1]. Therefore, it is important to create high concentration of NV^- centers considering the amount of P1 centers.

In current study, we investigate irradiation fluence dependence of the creation behavior of NV centers in type-Ib diamonds by using electron spin resonance (ESR) and photo-luminescence (PL) to understand the creation mechanism of NV^- center. The values of T_2 are also evaluated by Hahn-echo measurement, since it is one of the key parameters for highly sensitive magnetometry [1]. Then, we discuss the creation mechanism of NV centers based on concentrations of defects.

Method

The commercial diamonds synthesized by High Pressure and High Temperature (HPHT) were used. The initial P1 concentrations ($[P1]_{initial}$) for the samples were measured by ESR, 80, 72, 52, and 46 ppm, respectively. 2 MeV electrons were irradiated with fluences up to 8.0×10^{18} cm^{-2} at room temperature. Then, the samples were annealed at 1000°C for 2 hours to create NV centers. The concentration of P1 (number of electron spins) was measured by ESR. The initial concentration of P1 was in the range from 50 ppm to 100 ppm. The ratio of NV^- to NV^0 was evaluated from PL spectrum. All these measurements were performed at room temperature. The values of T_2 of NV^- center ensembles were measured using a home-built fluorescent microscope with a microwave system.

Results & Discussion

We studied the creation behavior of NV center in type-Ib diamonds with high $[P1]_{initial}$ under relatively high irradiation fluences. The decrease rate of P1 centers as a function of irradiation fluence shows similar tendencies for all type-Ib diamond samples, regardless of the initial P1 concentration in the low fluence range (~ 4.0×10^{18} e/cm^2). The reduction rate of P1 centers suggests that P1 centers are consumed by recombination with introduced vacancies. However, the decrease rate of P1 became lower in the high fluence ranges from 6.0×10^{18} e/cm^2 to 8.0×10^{18} e/cm^2, especially when $[P1]_{initial}$ is smaller, in spite that [P1] still exists even after irradiation at 8.0×10^{18} e/cm^2. The process of P1 center consumption seems to shift depending on the residual P1 centers. Furthermore, the P1 center consumption and NV^- center creation were compared and as a result, it is concluded that some amounts of the P1 centers were consumed by other defects. The conversion efficiency from $[P1]_{initial}$ to the $[NV^-]$ reached ~19% at 8.0×10^{18} e/cm^2 and the value confirms the usefulness of electron beam irradiation for high concentration of NV^- centers in type-Ib diamonds, whereas results in this study suggests that not all P1 centers converted to NV^- center and the residual defects might leads to a cause of decoherence..

Acknowledgement

This work was supported by Quantum Leap Flagship Program (Q-LEAP; JPMXS 0118067395 and JPMXS0118068379) of MEXT.

Reference

[1] J. F. Barry, J. M. Schloss, E. Bauch, M. J. Turner, C. A. Hart, L. M. Pham and R. L. Walsworth. Rev. Mod. Phys., **92**, No.1, 015004 (2020)

Synthesis of n-type diamond using *tert*-butyl phosphine for high sensitivity of the NV sensor

Riku Kawase[1], Hiroyuki Kawashima[1, 2], Hiromitsu Kato[2], Norio Tokuda[3], Satoshi Yamasaki[3], Mikihiro Kubota[1], Masahiko Ogura[2], Toshiharu Makino[2], Norikazu Mizuochi[1, 4]
[1]*Institute for Chemical Research, Kyoto University, Gokasho, Uji, Kyoto 611-0011, Japan*
[2]*National Institute of Advanced Industrial Science and Technology (AIST), Tsukuba, Ibaraki 305-8568, Japan*
[3]*Graduate School of Natural Science and Technology, Kanazawa University, Kanazawa, Ishikawa 920-1192, Japan*
kawase.riku.87n@st.kyoto-u.ac.jp

Introduction

Recently, ultra-long spin coherence time ($T_2 \approx 2.4$ ms) of the single nitrogen-vacancy (NV) center in P-doped n-type diamond was obtained[1]. The spin coherence time was the longest in room-temperature among solid-state systems. In addition to the long T_2, as a negative charge state of the NV center is stable[2]. Furthermore, it also reported that creation yield of shallow NV centers formed by ion-implantation was improved in addition to longer T_2 and improved charge stability[3]. Due to such reports, P-doping methods for n-type diamond synthesis is getting more important.

Phosphine is usually used for P-doped diamond synthesis by chemical vapor deposition (CVD). However, phosphine has high explosibility and toxicity, so it threatens safety of experimenters and expensive exclusion equipment was required. Therefore, we synthesized P-doped n-type diamond with *tert*-butyl phosphine (TBP) whose explosibility and toxicity were lower than phosphine's ones[4], and we confirmed that the synthesized sample shows relatively long T_2 (1620 ± 100 μs, FIG. 1). We also confirmed perfect alignment of NV axis which is also important for high sensitivity of NV quantum sensor.

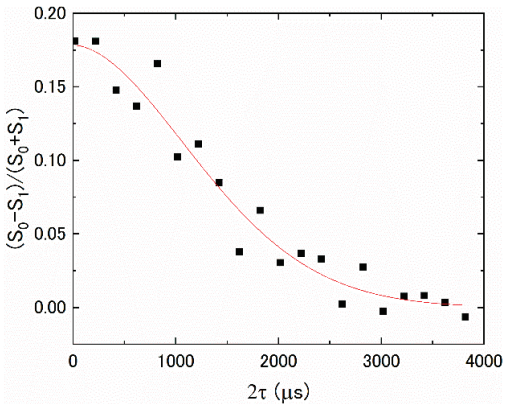

FIG. 1. Result of Hahn-echo measurement

Reference

[1]E. D. Herbschleb, H. Kato, Y. Maruyama, T. Danjo, T. Makino, S. Yamasaki, I. Ohki, K. Hayashi, H. Morishita, M. Fujiwara, N. Mizuochi, *Nature Communications*, **10**, 3766 (2019).
[2]Y. Doi, T. Fukui, H. Kato, T. Makino, S. Yamasaki, T. Tashima, H. Morishita, S. Miwa, F. Jelezko, Y. Suzuki, N. Mizuochi, *Physical Review B*, **93**, 081203(R) (2016).
[3]A. Watanabe, T. Nishikawa, H. Kato, M. Fujie, M. Fujiwara, T. Makino, S. Yamasaki, E. D. Herbschleb, N. Mizuochi, *Carbon*, **178**, 294-300 (2021).
[4]H. Kato, S. Yamasaki, and H. Okushi, *phys. stat. sol. (a)* **202**, 2122–2128 (2005).

This work was supported by MEXT Q-LEAP Grant Number JPMXS0118067395

Decoherence Phenomena in Nitrogen-Vacancy Diamond

Aulden Jones[1], Tokuyuki Teraji[2], Chikara Shinei[2], and Yuta Masuyama[3]
[1]*School of Physics, Georgia Institute of Technology*
[2] *Research Center for Functional Materials, National Institute for Materials Science*
[3]*National Institutes for Quantum and Radiological Science and Technology*

Introduction

Nitrogen vacancy (NV) centers in diamond are atom-sized spin defects whose unique properties enable their use as robust quantum sensors. Recent research efforts have focused on NV magnetometry, where both single and ensemble NVs are used for highly sensitive magnetic field detection with nanoscale spatial resolution. While NV sensors have been successfully applied to fields ranging from neuroscience to condensed matter physics, ensemble NV diamonds are still below the sensitivity threshold needed for many more potential applications[1]. Presented here is an attempt to investigate the relationship between large crystallographic strain features and the spin coherence time T_2^* in NV-diamonds grown by chemical vapor deposition (CVD). A better understanding of this relationship can provide valuable input for improving diamond growth methods and eventually extending T_2^*.

*This work was supported under the NSF Global Quantum Leap Program under Grant No. OISE-2020174.

Reference

[1]J. F. Barry, J. M. Schloss, E. Bauch, M. J. Turner, C. A. Hart, L. M. Pham, and R. L. Walsworth, Rev. Mod. Phys. 92, 015004 (2020).

Improvement in the long-term stability of the interferometer gyroscope using slow and continuous atomic beams

Naoki Nishimura[1], Takuya Kawasaki[2], Tomoya Sato[2], Ryotaro Inoue[2], Mikio Kozuma[1,2]
[1] *Department of Physics, School of Science, Tokyo Institute of Technology*
[2] *Institute of Innovative Research, Tokyo Institute of Technology*
nishimura.n.ae@m.titech.ac.jp

Introduction

Gyroscopes consisting of an atom interferometer can measure angular velocity. Since their expected sensitivity is higher than that of optical interferometers [1], many studies have paid much attention to the application of atom gyroscopes, for example, precision measurement of physical constants [2] and inertial navigation of ships and aircraft [3]. We are developing a matter-wave gyroscope using Raman transitions for a cold and continuous Rb atomic beam. A deadtime-free measurement and long-stability obtained by a continuous atom beam interferometer benefit the non-GPS type of inertial navigation. In our previous study, we successfully measured the rotation of the Earth with our gyroscope with continuous and cold atomic beam of Rb [4]. Currently, we are aiming to improve the accuracy of the gyroscope for the level required for inertial navigation.

Method

In the atom interferometer using Raman transitions, three pairs of counter-propagating Raman beams construct a π/2-π-π/2 Mach-Zehnder type interferometer [5]. The phase in the interference signal, which reflects the Sagnac effect, is measured as the population ratio between the ground-state hyperfine states F=1 and F=2 of ^{87}Rb atom. The constant frequency shift Δf in the π Raman beams induces a sinusoidal change in the ratio of the population with the frequency of $2\Delta f$. We create a reference signal of the frequency $2\Delta f$ based on the signal of the frequency Δf by a synthesizer. We estimate the phase of the fluorescence signal by the lock-in detection with the reference signal.

If drift occurs in the relative phase of Raman beams, it worsens the long-term stability of the interferometer. To eliminate the spurious phase shift caused by the drift in the relative phase of Raman beams, a simultaneous measurement of interferometers with counter-propagating atomic beams that share Raman beams is employed. The sign of the Sagnac phase shift induced by the rotation depends on the velocity vector, while that induced by other drifts such as acceleration, movement of optical elements, and imperfections in the equipment is the same for the interferometers. Thus, the common-mode phase drifts are canceled by taking the difference between the output phase shifts in two interferometers while enhancing the phase shift originating from the system's rotation. Although the common-mode rejection is a powerful method to improve long-term stability, the common-mode rejection ratio is limited in the actual system. It is desirable to suppress the relative phase drift itself as much as possible. One of the most significant sources of long-term drift in the output phase of our interferometer is the imperfectness in the relative phase locking of Raman beams. The relative phase of counter-propagating Raman beams is measured as the optical beat note between Raman beams. The locking of the relative phase is achieved by stabilizing the beat note to the external RF reference using the PID feedback loop. The performance of the feedback circuit, which consists of discrete electronic components, is vulnerable to changes in operational conditions, such as temperature. We newly introduce the feedback circuit consisting of a field programmable gate array (FPGA). The full-digitalized feedback system is free from the instability stemming from the change in the environmental conditions where the gyroscope is operated. As a result, the performance of the stabilization of the relative phase of Raman beams is improved.

Result

The stability of the interferometer as a gyroscope is evaluated by calculating the Allan deviation of the output phase of the interferometer. The performance of the gyroscope with FPGA-based stabilization for the relative phase of Raman beams will be reported. In addition, the changes in the response of the interferometer to the variations in the environmental condition will be presented.

Reference

[1]T. L. Gustavson, P. Bouyer, and M. A. Kasevich, *Phys. Rev. Lett*, 78, 2046 (1997)
[2]G. Rosi, F. Sorrentino, L. C Acciapuoti, M. P Revedelli, G. M. Tino. *Nature*, 510, 518-521 (2014)
[3]J.C. Fang and J. Qin *Sensors*, 12, 6331-6346 (2012)
[4]T. Sato, R. Inoue and M. Kozuma, short presentation in 4th IFQMS, SE-03A-δ1-05, 7-9 Dec. 2021
[5]M. Kasevich and S. Chu, *Phys. Rev. Lett*, 67, 181 (1991).

Bragg interferometer using slow and continuous atomic beam with sub-recoil transverse momentum width

Tomoya Sato[1], Toshiyuki Hosoya[2,3], Ryotaro Inoue[1] and Mikio Kozuma[1,3]
[1] *Institute of Innovative Research, Tokyo Institute of Technology*
[2] *Japan Aviation Electronics Industry, Ltd.*
[3]*Department of Physics, School of Science, Tokyo Institute of Technology*
sato@qnav.iir.titech.ac.jp

Introduction

A gyroscope based on interferometry using a continuous atomic beam is one of the most promising candidates for next-generation inertial navigation to complement navigation with external references such as GPS because of their high sensitivity, deadtime-free detection, and long-term stability. In recent years, alkaline earth-like atoms have attracted attention to improving the sensitivity and stability of interferometers [1]. In contrast to alkali atoms, which are widely used in atom interferometry [2], alkaline earth-like atoms do not possess electron spin in their ground state, making them less susceptible to effects of environmental magnetic fields. An interferometer with Bragg diffraction, which uses only the ground state, can benefit from this advantage. In addition, higher-order Bragg diffraction increases the area of the interferometer, thus the sensitivity of the gyroscope will be improved.

In atomic interferometry with Bragg diffraction, the interference signal is evaluated by measuring the number of atoms in different momentum states of the same internal state. Therefore, an atomic beam whose initial momentum width is narrower than the recoil momentum of the Bragg beam is essential for high-precision measurement. In our recent paper, we propose a new technique to obtain the high-flux atomic beam of ytterbium (Yb) with sub-recoil momentum width [3]. The interferometer with such type of atomic beam will pave the way to the high-end gyroscope for inertial navigation.

Method

By applying two-dimensional cooling using $^1S_0$-$^3P_1$ intercombination transition to a slow atomic beam of ^{171}Yb produced by dipolar-allowed transition, we have successfully compressed the transverse momentum width of the atomic beam to below $4\hbar k$, where $\hbar k$ is the recoil momentum of the Bragg beam (dipolar-allowed $^1S_0$-$^1P_1$ transition). For further reduction of momentum width, we applied a momentum filtering technique to our atomic beam using an ultra-narrow transition between the ground state and long-lived metastable state $^3P_2$. The atomic beam orthogonally passes the laser light resonant on the ultra-narrow transition (507nm). With our experimental condition, the spectral linewidth associated with the transverse momentum width of the atomic beam is determined by the transit time broadening rather than the lifetime of the metastable state. Since the transition time broadening is adjusted to correspond to the momentum width of less than $\hbar k$, atoms can be excited to the metastable state in a momentum-selective manner. After blowing up the remaining atoms in the ground state, which have unwanted momentum components, one can obtain ground state atoms within the narrow momentum width by transporting the atoms from the metastable state to the ground state in the same momentum-selective manner.

The momentum-filtered atomic beam is introduced into the interferometer region, where three pairs of counter-propagating Bragg beams construct the π/2-π-π/2 Mach-Zehnder type interferometer. The Sagnac effect causes the sinusoidal variation between populations of momentum states $0\hbar k$ and $2n\hbar k$ as a function of the acceleration and angular velocity on the Sagnac loop, where n is the order of the Bragg diffraction. For the momentum-resolved detection, the third 507nm light, tuned to excite the $2n\hbar k$ state, is introduced just after the interferometer. The change in the population of the $2n\hbar k$ momentum state can be detected as the change in the loss of the atoms in the ground state.

Results

We successfully generate an atomic beam of ^{171}Yb whose momentum width is $0.20(8)\hbar k$ by the momentum filtering. The higher order Bragg diffraction, up to the 10th, is observed. With the obtained atomic beam with narrow momentum width, the construction of the Bragg interferometer is ongoing. The present status of the development will be reported.

This work was supported by JST-Mirai Program, Grant Number JPMJMI17A3 and COI-NEXT, Grant Number JPMJPF2015.

Reference

[1]T. Mazzoni et al., *Phys. Rev. A*, 92, 053619 (2015).
[2]D. Sayoie et al., *Sci. Adv.* 4, eaau7945 (2018).
[3] T. Hosoya et al., *Opt. Commun.*, 528, 129048 (2023).

Development of a cryogenic suspension system for TOrsion-Bar Antennae (TOBA)

Ching Pin Ooi[1], Satoru Takano[1], Yuka Oshima[1], Kentaro Komori[2], Yuta Michimura[2,3] and Masaki Ando[1,2]

[1]*Department of Physics, The University of Tokyo*
[2]*RESCEU, The University of Tokyo*
[3]*LIGO Laboratory, California Institute of Technology*
ooichingpin@g.ecc.u-tokyo.ac.jp

Introduction

TOrsion-Bar Antennae (TOBA), is a proposed gravitational wave antenna[1], targeted at observing intermediate mass black hole mergers with peak sensitivity in the range 0.1 – 10 Hz, but can also be used for early earthquake warnings via measuring transient gravitational perturbations[2]. TOBA phase III is currently being built, with a target sensitivity that would make it useful for early earthquake warnings. To that end, a cryogenic suspension system is being developed to achieve the low thermal suspension noise requirements. TOBA, as its name suggests, uses torsion bars for sensing. Thus, this work focuses on quantifying and reducing suspension thermal noise of torsion pendulums, with two key technologies, cryogenic temperatures and crystalline fibres.

Method

Our setup consists of a copper beryllium torsion pendulum, suspended by a 1 mm thick sapphire fibre, and is cooled in a cryogenic chamber to near 4 K. The Q value, a parameter which characterizes the thermal noise of the suspension, is measured off the setup via an optical lever. Coil-coil actuators were used to excite the torsion pendulum to start off the ringdown for Q value measurements.

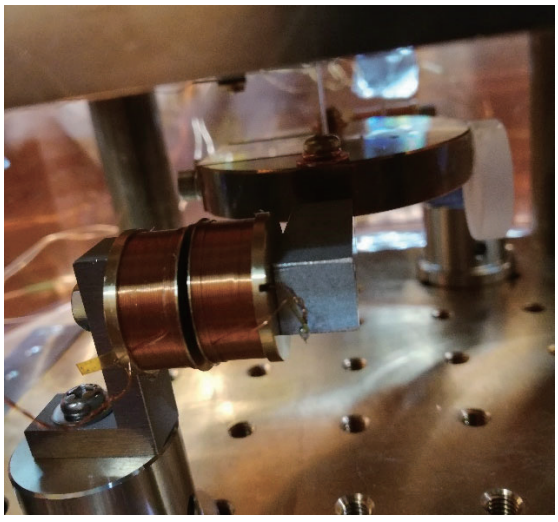

Fig. 1. Torsion pendulum suspended by 1 mm sapphire fibre, in a cryogenic chamber. Coil-coil actuators provide the initial excitation for ringdown.

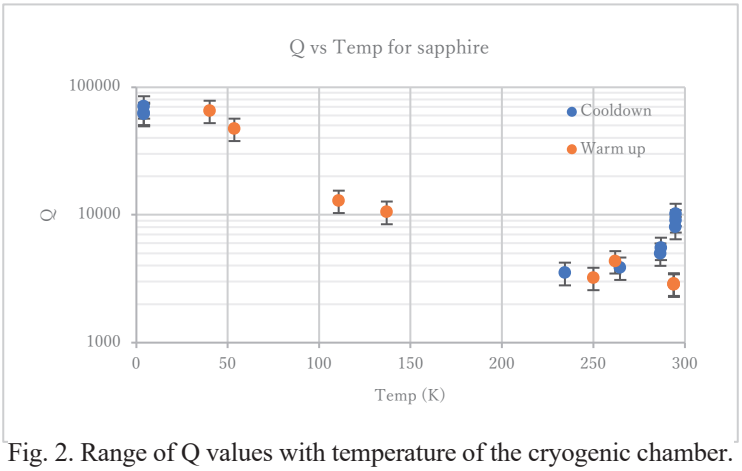

Fig. 2. Range of Q values with temperature of the cryogenic chamber. This ranges from 3000 – 70 000 across the temperatures, and we note here that the highest values are when it is coldest.

Acknowledgments

We would like to thank the Shigemi Otsuka and Togo Shimozawa for manufacturing the mechanical parts used.
This work is supported by MEXT Q-LEAP Grant Number JPMXS0118070351.

Reference

[1]M. Ando *et al.*, *Phys. Rev. Lett.*, 105, 161101 (2010)
[2]J. Harms *et al.*, *Geophys. J. Int.*, 201, 1416-1425 (2015)

Torsion-Bar Antenna for Early Earthquake Alert

Yuka Oshima[1], Satoru Takano[1], Ching Pin Ooi[1],
Kentaro Komori[2], Yuta Michimura[2,3], and Masaki Ando[1,2]
[1]*Department of Physics, University of Tokyo*
[2]*RESCEU, University of Tokyo*
[3]*LIGO Laboratory, California Institute of Technology*
yuka.oshima@phys.s.u-tokyo.ac.jp

Introduction

Torsion-Bar Antenna (TOBA) is a highly sensitive gravity gradient sensor using torsion pendulums [1]. We use test masses suspended horizontally and aim to detect the torsional rotation caused by tidal forces as shown in FIG. 1. The resonant frequency of torsional motion is ~1 mHz, therefore TOBA has good design sensitivity in low frequencies (0.1 – 10 Hz). TOBA is useful for gravity-based earthquake early warning [2], and the observation of Newtonian noise and gravitational waves. A prototype detector Phase-III TOBA with a 35 cm-scale pendulum is under development [3]. The target sensitivity is set to 10^{-15} /√Hz at 0.1 Hz. Phase-III TOBA can detect earthquakes with a magnitude 7 or larger within 10 seconds from a 100 km distance [3].

Method

For Phase-III TOBA, we operate torsion pendulums at cryogenic temperatures to reduce thermal noise. We have successfully demonstrated cooling down test masses at 6 K [4]. Now, torsion pendulums are under development to achieve our target sensitivity. Differential Fabry-Perot cavities are used to read out the rotational angle to the pendulums. We finished designing the parameters of Fabry-Perot cavities and the mechanical parts for the pendulums.

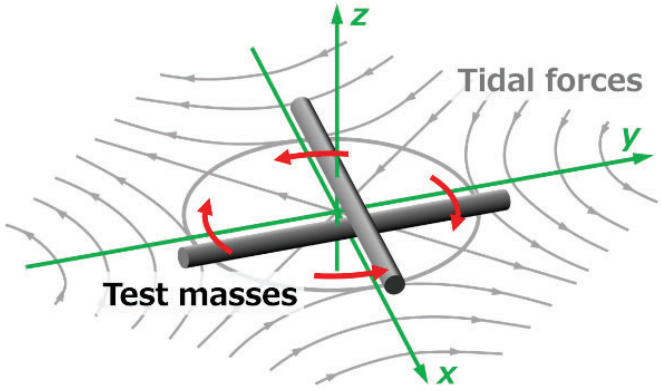

FIG. 1. the schematic of TOBA. Test masses are suspended horizontally in the x-y plane and a suspension wire is stretched in the z-axis. Grey lines represent tidal forces, red arrows show the rotational motion of the pendulums.

Acknowledgments

We would like to thank Shigemi Otsuka and Togo Shimozawa for manufacturing the mechanical parts used. This work was supported by MEXT Quantum LEAP Flagship Program (MEXT Q-LEAP) Grant Number JPMXS0118070351. Y.O. was supported by JSPS KAKENHI Grant Number JP22J21087 and JSR Fellowship, the University of Tokyo.

Reference

[1]M. Ando *et al.*, *Phys. Rev. Lett.*, 105, 161101 (2010).
[2]J. Harms *et al.*, *Geophys. J. Int.*, 201, 1416 (2015).
[3]T. Shimoda *et al.*, *International Journal of Modern Physics D*, 29, 1940003 (2020).
[4]T. Shimoda, PhD thesis, The University of Tokyo (2019).

Optimized Design of Quasi-phase-matched crystal for Spectrally-Pure-State Generation at MIR Wavelengths Using Metaheuristic Algorithm

Wu-Hao Cai, [1, 2, *], Fumihiro Kaneda, [1] Keiichi Edamatsu, [1] and Rui-Bo Jin[2, *]

[1]*Research Institute of Electrical Communication, Tohoku University, 2-1-1 Katahira, Sendai, 980-8577, Japan*

[2]*Hubei Key Laboratory of Optical Information and Pattern Recognition, Wuhan Institute of Technology, Wuhan 430205, China*

[*]*E-mail: cai@quantum.riec.tohoku.ac.jp; jin@wit.edu.cn*

Introduction

Quantum light sources in the mid-infrared (MIR) band play an important role in many applications, such as quantum sensing, quantum imaging, and quantum communication. However, there is still a great demand for high-quality quantum light sources in the MIR band, such as the spectrally pure single-photon source. In this work, the generation of a spectrally-pure state in an optimized poled lithium niobate crystal using a metaheuristic algorithm is presented. In particular, the particle swarm optimization algorithm is adopted to optimize the duty cycle of the poling period of the lithium niobate crystal. With this approach, the spectral purity can be improved from 0.820 to 0.998 under the third group-velocity-matched condition, and the wavelength-tunable range from 3.0 to 4.0 μm for the degenerate case and 3.0 to 3.7 μm for the nondegenerate case. This work paves the way for developing quantum photonic technologies at the MIR wavelength band [1-4].

Tables and Figures

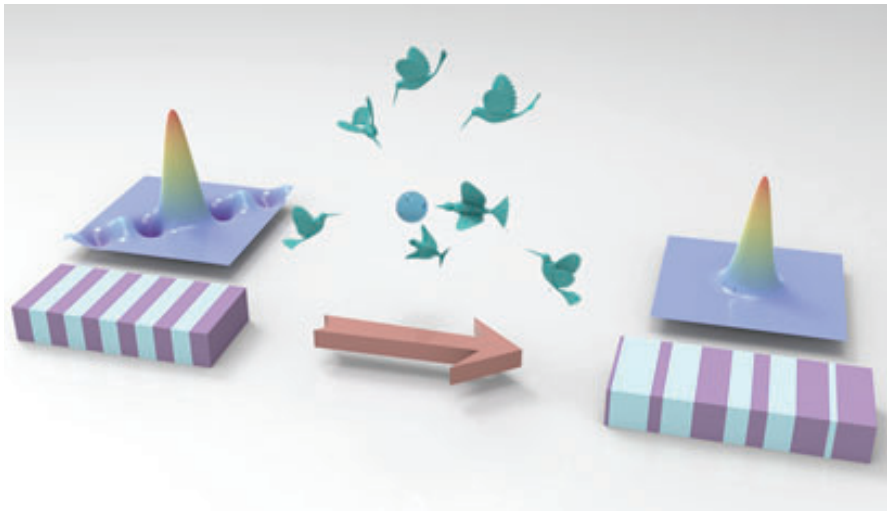

FIG. 1. The concept figure of optimized design of the lithium niobate crystal by using particle swarm optimization (PSO) algorithm. Left: In a standard periodically poled lithium niobate crystal, side lobes in the joint spectral amplitude (JSA) profile of biphoton degraded the purity. Right: In an optimized poled LN (OPLN) crystal which is designed using a PSO algorithm, the side lobes can be eliminated after optimization, the spectral purity of JSA can be improved obviously.

Reference

[1]W.-H. Cai, Y. Tian, S. Wang, Q. Zhou, C. You*, and R.-B. Jin*, *Adv. Quantum Technol.,* 5, 2200028 (2022) **Selected the front cover of the journal for the July issue**

[2]B. Wei, W.-H. Cai, C. Ding, G.-W. Deng, R. Shimizu, Q. Zhou, R.-B. Jin, *Opt. Express,* 29, 256 (2021).

[3]P. B. Dixon, J. H. Shapiro, F. N. C. Wong, *Opt. Express*, 21, 5879 (2013).

[4]C. Cui, R. Arian, S. Guha, N. Peyghambarian, Q. Zhuang, Z. Zhang, *Phys. Rev. Appl.*, 12, 034059 (2019)

Experimental generalized measurement of qubits using a quantum computer

Tingrui DONG[1,2], Binho LE[3], Fumihiro KANEDA[1], Soyoung BAEK[1] and Keiichi EDAMATSU[1]
[1]*Research Institute of Electrical Communication, Tohoku University*
[2]*School of Engineering, Tohoku University*
[3]*Frontier Research Institute for Interdisciplinary Sciences, Tohoku University*
dong.tingrui.r7@dc.tohoku.ac.jp

Introduction

Quantum computers, which provide the ability to surpass classical computers, are also able to carry out some fundamental experiments in quantum mechanics. For example, generalized quantum measurement protocols and their uncertainty relations[1] [1] can be realized and tested in a quantum computer. Here, we propose the implementation of generalized quantum measurement of qubits in a noisy intermediate-scale quantum computer (NISQ). First, we demonstrate the variable-strength measurement of a single qubit, which was once studied by photon polarization qubits[2], using an NISQ (IBM-Q). The performance of the measurement is quantified and discussed in terms of the characteristics of the noise and error of the NISQ. We also implement the nonlocal, variable strength parity measurement of a pair of qubits we recently proposed[3]. The circuit we build will also be a part of deterministic, complete Bell state measurement with arbitrary precision. To date, we made a demonstration of the strongest measurement situation by using the 7-qubit quantum computer (ibm-perth). The performance of the measurement strategy is limited due to the noise and error in present NISQ.

This work is supported by MEXT Q-LEAP (JPMXS0118067581) and JST, the establishment of university fellowships towards the creation of science technology innovation (JPMJFS2102).

Figures

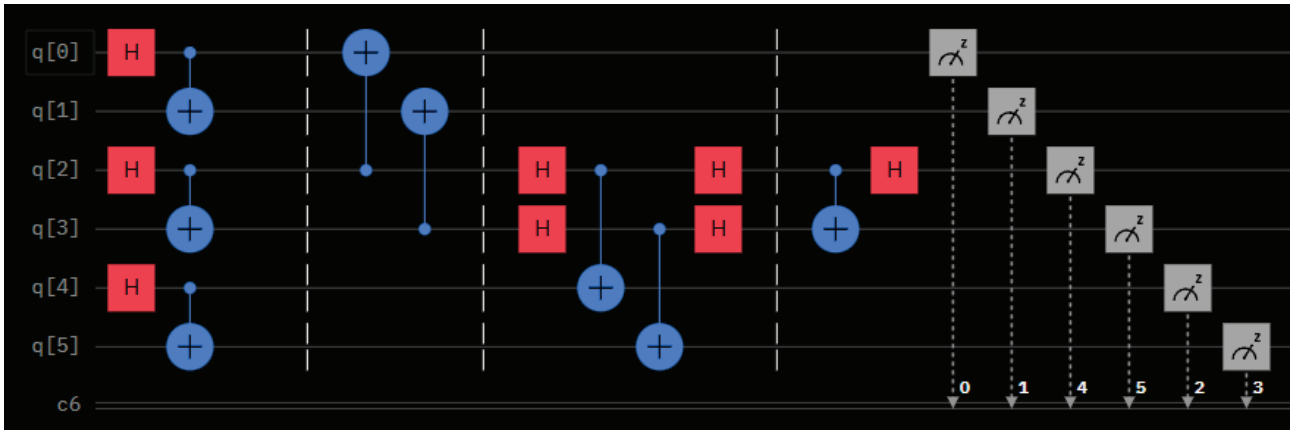

Fig.1 The measurement circuit of measuring a pair of qubits. The qubit 0 and 1 perform as meter 1 for measurement parity information. The qubit 2 and 3 perform the entangled system. The qubit 4 and 5 perform as the other meter for checking the phase information. The system pair is coupled with two meters by CNOT gate. Finally, the Bell-state measurement are done on the system qubits, and the meters are projected on the calculational basis.

Reference

[1]M. Ozawa, Phys. Rev. A, 67, 042105 (2003).
[2]F. Kaneda, S.-Y. Baek, M. Ozawa, and K. Edamatsu, Phy. Rev. Lett. 112, 020402 (2014).
[3]P. Vidil and K. Edamatsu, New J. Phys. 23, 043004 (2021).